CHIMIKA CHRONIKA

NEW SERIES

AN INTERNATIONAL EDITION
OF THE ASSOCIATION OF GREEK CHEMISTS

CMCRCZ 20(1), 3-64(1991)

ISSN 0366-693X

1-2/91

Volume 20, No 2p.p. 3-64 March 1991

CHIMIKA CHRONIKA
NEW SERIES
AN INTERNATIONAL EDITION

Pubished by the Association of Greek Chemists (A.G.C.)
27 Kaningos str. Athens 106 82 Greece

Correspondence, submission of papers, subscriptions, renewals and changes of address should be sent to Chimika Chronika-New Series, 27 Kaningos street, Athens 106 82, Greece. The Guide to Authors is published in the first issue of eaech volume, or sent by request. Subscriptions are taken by volume at 1000 drachmas for membres and 2000 drachmas for Corporations in Greece and 28 U.S. dollars to all other countries except Cyprus, where subscriptions are made on request.

Phototypesetted and Printed in Greece by LICHNOS LTD GRAPHIC ARTS
24, PL. THEATROU 105 52 ATHENS tel. 3214766

Υπεύθυνος σύμφωνα με το νόμο: Νίκος Κατσαρός, Κάνιγγος 27, Αθήνα 106 82.

Responsible under law: Nikos Katsaros, 27 Kaningos St, Athens 106 82, Greece.

GUIDE TO AUTHORS

Since January 1,1988, all contributions to Chimika Chronika, New Series are reproduced from camera-ready typescripts prepared by the authors.

Scope and Editorial Policies. — This International edition invites original contributions on research in all branches of chemistry and related sciences at the molecular level. Negative results will only be accepted when they can be considered to contribute significantly by the science. In the selection by the editors of manuscripts for publication, emphasis is placed on the quality and originality of the work.

Papers should be written in English. Authors need not be members of the Greek Chemists Association.

Manuscripts are classified as (normal length) *papers, short papers* or *notes, preliminary communications or letters, and reviews. A short paper* is a concise but complete description of a small, rounded off investigation or of a side part from the main line of investigation, which will not be included in a later paper. It is not a portion of work, that can be more suitably incorporated in a normal length paper, after the investigation has progressed further.

As *Notes* are characterized short papers on limited facets of an investigation e.g. describing a useful modification of an experimental technique or method, reporting additional data and eventually, more precise values for measurements already existing in the literature, and so on.

A *Preliminary Communication* is a brief report of work, which will be included in a later normal length paper. Criteria for its publication are first, when it is considered that the science would be advanced if results were made available as soon as possible to others working on the same subject and second, for the protection of priority for the author. Every effort is made in order to publish preliminary communications as soon as possible and it would help the editors if the author, in a covering letter, were to give his reasons for believing that publication is urgent. Although extensive references to the earlier literature are not usually needed, the most recent papers on the same subject should be referred to, and sufficient experimental details should be given so that those familiar with the subject can immediately repeat the experiments. In general, preliminary communications should be more than an abstract or a summary.

As *Letters* are characterized any other types of communications, previously included in the terms "letter to editor" or "communication to editor", but not fulfilling the criteria mentioned above for a preliminary communication or a note, or dealing with scientific criticism of published work in this (or other) journals.

Reviews should be fully comprehensive on a narrow field of specialized research, expected to be interesting for a broad number of scientists: they are invited papers, otherwise submitted after contracting the editors.

Organization of Manuscripts. — Athors should submit *three copies* of the manuscript in double-spaced typing on the one side of pages of uniform size, with a margin 5 cm wide on the left; this applies also to summaries (english and greek), references and notes.

Every manuscript should begin with a *Cover Page* and attached to it on a separate sheet, the *Acknowledgments* and notice of grant support (if appropriate).

The cover page should contain the title, the name(s) of author(s) (first-name in full, middle, surname), the name and address of laboratory of research, the footnotes to the title and/or to an author's name (both made with asterisks), and the name and address of the recipient correspondence. It should also contain a Running Title, not exceeding 40 letters.

The purpose of this arrangement is to facilitate the reviewing procedure, which is based on a protective anonymity between reviewers and authors, closen in order to meet the requirements of a highly objective selection of papers to be published in this journal, and to increase the validity of criticisms. Cover page and aknowledgements are not sent to reviewers and accordingly, sentences in firs person accompanied by literature references to earlier papers of the author(s) should be completely avoided in the text.

The next pages of the manuscript should be numbered in one consecutive series by the following sequence:

Page 1. — *Title* followed by a *summary* in English. The title should consist of carefully selected and properly presented key words which clearly identify the subjects considered in the paper. The *summary* should be as brief as possible but intelligible in itself, without reference to the paper, and containing sufficient information to serve as an *abstract.*

Every *summary* should end with up to ten *key words,* necessary to direct the attention of abstracting services and readers to subjects in the article that are not referred to in the title.

Page 2. — *Abbreviations* and *Terminology,* i.e. a list of all abbreviations and unusual terms used in the paper; it may include the systematic name of any compound, mentioned in the text by a shorter "trivial" or "common" name.

Page 3 and subsequent. — The text divided into sections and, if necessary, subsections. The first section of a normal-length paper is always an *Introduction* stating the reasons for performing the work, with brief reference to previous work on the subject; the background discussion should be restricted to pertinent material, avoiding an extensive review of prior work; and documentation of the literature should be selective rather than exhaustive, particularly if reviews can be cited.

The arrangement of the text after the introduction is left to the author(s). The order *Materials, Methods, Results and Discussion,* with headings, subheadings and sideheadings chosen by the author(s), is usually the most satisfactory. However, in lengthy papers (usually, of synthetic work) the manuscript may be organized so that the principal findings and conclusions are concisely presented in an initial section (Theoretical Part), with supporting data, experimental details, and supplementary discussion in a separate section (Experimental Part).

Photocopies of tables, figures, legends, footnotes etc should be pasted on the appropriate place, so that each page will be ready for reproduction. The size of letters chosen for the original should be legible after 20% reduction during reproduction.

Subsequent Pages — After the text pages separate sheets should be used for the following: a) greek summary; b) references and notes.

The *greek summary,* headed by a greek translation of the title, should be extensive and may refer to literature citations and to tables or figures of the paper, in order to give a brief but factual account of the contents and conclusions of the paper, and of its relevance; for this purpose, it may exceed half printed page. In its place, foreign authors may submit an extensive summary in english, which will be gladly translated into greek by care of the editors.

References and Notes, as already mentioned, should be brought together at the end of the paper in one consecutive series by order of citation in the text (not in alphabetical order). Authors should check whether every reference in the text appears in the list and *vice versa.* References to papers "in press" imply that the paper has been accepted for publication and, therefore, the name of the journal should be given. References to a "personal communication" (never "private") will be accepted only when the author submits written permission of the worker concerned. References should be listed according to the following style:

For journal articles: Last name(s) of author(s) and initials: *Name of journal* (abbreviated according to Chemical Abstracts, Service Source Index (CASSIS) 1907-1984, *Volume number,* First page of article, Year in parentheses.

Example: 1 Smith, J.B. and Jones, A.B.: *J. Am. Chem. Soc.* **47,** 115 (1945).

For books and monographs: Author's names as above: *Title of book,* (Number of edition), Page, Publisher, City, Year of edition.

Example: 2 Smith, J.B.: *Organic Chemistyr,* (2d edition), p. 57, Wiley, London (1945).

For multi-author volumes (Articles in books): Authors' names as above: Name of editor(s): *Name of book* Volume number Part number, Page(s), Publisher, City, Year of edition.

Example: 3 Smith, J.B.: Jones, A.B.: *Organic Chemistry,* Vol. 5. Part A, p. 57 (or pp. 46-62), Elsevier, Amsterdam, 1953.

Manuscripts for short papers and preliminary communications should be organized on the same principles. Besides some minor modifications in their published form, they differ from a normal length paper in that the headings and subheadings in the text, as well as the summary preceeding the text are ommitted. In these cases, the first paragraph of the text may serve the purpose of an abstract, summing up very briefly the scope and the main findings and conclusions of the investigation. However, for reasons already mentioned, the text is always followed by a greek extensive summary.

After the paper is accepted for publication it is returned to the authors for the preparation of the final camera ready typescript. The authors are required to prepare the typescript on a special paper supplied by the Editing Commitee according to enclosed instructions.

Page Charge and Reprints. A page charge of 2000 drachmas or 20 U.S. dollars assessed to cover in part the cost of publication, plus the cost of 50 reprints, which will be mailed to the recipient correspondence without any additional requirement. However, papers are accepted or rejected only on the basis of merit and the decision to publish a paper is made before the charge is assessed.

Chimika Chronika, New Series, 20, 3-15 (1991)

ÉTUDE CINÉTIQUE DE L'ADSORPTION DU MEOH SUR Pt POLYCRISTALLIN

A. PAPOUTSIS et G. PAPANASTASIOU

Laboratoire de Chimie Physique de la Faculté des Sciences de l'Université de Thessalonique, 540 06 Thessalonique Grèce.

(Received July 20, 1989)

SOMMAIRE

La cinétique d'adsorption du MeOH sur Pt lisse a été étudiée en utilisant des données tirées par la méthode de la voltammetrie cyclique programmée. La capacité des modèles Langmuir et Temkin à décrire le phénomène a été testée. Il est mis en evidence que le modèle Langmuir est en général insuffisant pour décrire l'adsorption du methanol. En revanche, le modèle Temkin a été prouvé très adequat dans le cas où $C_{MeOH} = 0,1M$ et jusqu'à $\theta \approx 0,5$.

L'application du modèle Temkin aux concentrations 0,01 et 1,0M en MeOH montre que dans ces conditions ce modèle est insuffisant à décrire le phénomène global.

Key words: adsorption, adsorption of methanol on Pt, adsorption isotherms, adsorption kinetics.

INTRODUCTION

L'oxydation électrocatalytique du MeOH sur des électrodes métalliques a été étudiée exhaustivement par plusieurs chercheurs les vingt dernières années puisque il s'agit d'un combustible, utilisé aux piles à combustible, très attractif pour des raisons diverses (rendement d'énergie élevé, bas prix, produit de combustion non polluant [1]). Le mécanisme de la réaction d'oxydation du MeOH reste encore un object de recherche et de controverses. Parmi les obstacles les plus importants à l'élucidation du phénomène global est la connaissance de l'identité des espèces intermédiaires, qui se forment à l'étape de la chimisorption dissociative du MeOH. Certains espèces s'adsorbent très fortement et empoisonnent

la surface de l'électrode. Les espèces intermédiaires possibles provenantes de la chimisorption dissociative du MeOH sont les suivantes:

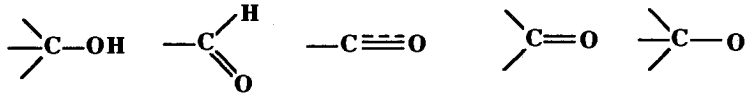

Par ailleurs, il est evident que des informations intéressantes peuvent être tirées d'une étude de la cinétique d'adsorption du MeOH sur la surface de l'électrode, surtout en ce qui concerne l'isotherme d'adsorption suivie et, par conséquence, la nature des forces entre les espèces adsorbées.

M. Breiter était le premier qui a étudié la cinétique d'adsorption du MeOH sur Pt lisse [2]. Cependant, ses conclusions concernant la vitesse d'adsorption sont tirés à partir de données indirectes obtenues dans des conditions non stationnaires.

Bagotsky et ses coll. ont étudié plus systématiquement l'adsorption du MeOH et sa cinétique, en milieu acide (1M H_2SO_4), sur Pt lisse ainsi que sur Rh et Ir [3,4,5] en utilisant une méthode de pulses cathodiques et anodiques. Ils ont montré que pour des concentrations de MeOH supérieures à 10^{-3}M la vitesse d'adsorption est considérablement plus basse que la vitesse de la diffusion vers la surface de l'électrode. Par conséquent, l'adsorption constitue l'étape déterminante de la vitesse de la réaction. Ils ont aussi constaté que l'adsorption du MeOH, dans le cas où l'adsorption est déjà arrivée à l'état d'équilibre (état de saturation), peut être representée par l'isotherme de Temkin connue comme isotherme d'équilibre:

$$\theta = a + \frac{1}{f} \ln C \qquad (1)$$

où a désigne une constante, θ le degré de recouvrement de la surface de l'électrode par les intermédiaires adsorbées du methanol et f un facteur associé à la hétérogéneité de la surface exprimant la différence entre la valeur maximum (ΔG_{max}) et minimum (ΔG_{min}) de l'énergie libre d' adsorption:

$$f = \frac{\Delta G_{max} - \Delta G_{min}}{RT}$$

Il est à noter que ΔG_{min} représente l'énergie libre d'adsorption quand $\theta \rightarrow 0$, tandis que ΔG_{max} est l'énergie libre d'adsorption quand θ atteint sa valeur de saturation.

En ce qui concerne la cinétique d'adsorption du MeOH ils ont constaté que θ varie linéairement en fonction du logarithme du temps d'adsorption, c'est à dire

$$\theta = A + \frac{1}{\alpha f} \ln t \qquad (2)$$

A étant une constante et α un paramètre dont les valeurs se trouvent dans l'intervalle $0<\alpha<1$. Cette équation est connue comme isotherme cinétique d'adsorption. La vitesse d' adsorption

pour θ = constant est directement proportionelle à la concentration (molarité) du MeOH au sein de la solution et le logarithme de la vitesse d'adsorption diminue linéairement avec l'augmentation du degré de recouvrement de la surface θ. Ainsi, la vitesse d'adsorption v_{ads} du MeOH sur platine lisse à un potentiel constant est representée par l'équation de Roginskii-Zel'dovich

$$v_{ads} = \frac{d\theta}{dt} = k_{ads} C \exp(-\alpha f \theta) \qquad (3)$$

où la vitesse specifique de la réaction d'adsorption k_{ads} reste constante.

Plus recement Sokolova et coll. [7] ont examiné l'adsorption du MeOH en utilisant les modèles de Temkin et Langmuir; en admettant que le methanol chimisorbé occupe 1, 2 ou 3 sites d'adsorption ils ont constaté que leurs résultats expérimentaux s'adaptent aux équations respectives. Il est toutefois à noter que ces résultats expérimentaux n'étaient pas suffisamment nombreux et par conséquent il est très difficile d'affirmer si les équations utilisées decrivent en réalité le phénomène. En plus, les temps d'adsorption t utilisés sont assez longs (t > 10 sec), de sorte que le recouvrement de la surface de l'électrode arrive, dans tout les cas, pratiquement à l'état de saturation.

Peu de travail a été fait à l'égard d'une approche absolument théorique concernant le problème de la cinétique d'adsorption des substances organiques sur des électrodes solides [8,9].

PARTIE EXPÉRIMENTALE

Les valeurs de θ utilisées dans ce travail ont été obtenues en utilisant la méthode de la voltammetrie cyclique programmée déjà décrite [10,11]. Toutes les mesures expérimentales ont été réalisées au laboratoire de Chimie I (Électrochimie et Interactions) de l' Université de Poitiers à l'aide d'un montage électronique totalement controlé (piloté) par un micro-ordinateur. Dans la figure 1 nous donnons à titre d'exemple un couple de voltammograms cycliques en presence et en absence du MeOH. Dans cette figure les corrections effectuées concernant la couche double sont schematiquement indiquées. Mais les détails de la determination de θ ont été déjà décrits [11].

Le montage utilisé présente deux avantages importants:

1) Possibilité de déterminer le paramètre θ à des temps très courts (t < 10 sec).

2) Absence d'intervention d'expérimentateur lors de la réalisation d'une expérience d'adsorption, un avantage qui augmente la précision et la reproductibilité des résultats.

Ces avantages nous ont donné la possibilité d'ajuster des équations polynômiales avec les courbes d'adsorption expérimentales de sorte que la cinétique d'adsorption soit quantativement suivie.

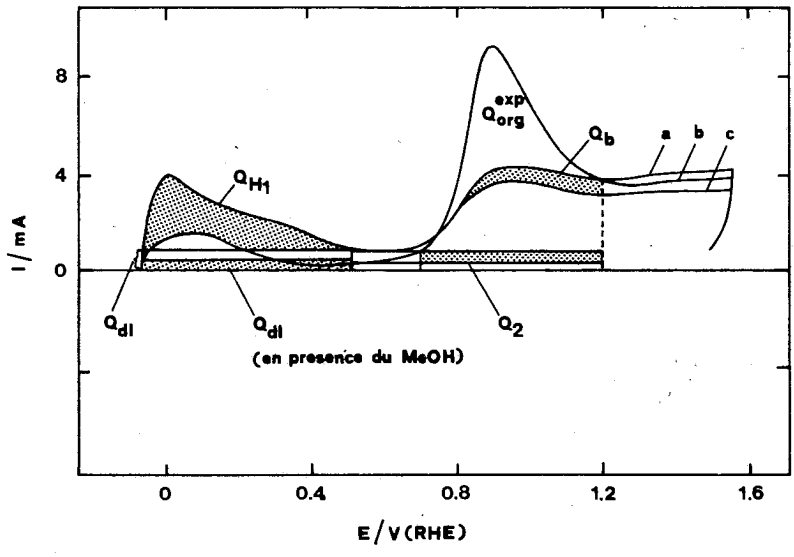

Fig. 1. Voltammogrammes cycliques de l'adsorption du MeOH sur Pt lisse en milieu $HClO_4$ 0,5M. Vitesse de balayage 50V/s. Potentiel d'adsorption 0,4V/RHE. a) C_{MeOH} = 0,1M t_{ads} = 60s b) C_{MeOH} = 0,1M t_{ads} = 0.0s (cyclage continu) c) C_{MeOH} = 0,0M t_{ads} = 0,0s. Les parties ombrées, Q_{H1}, Q_{dl}, Q_2, Q_b sont les differentes quantités d'électricité utilisées pour la réalisation de corrections nécessaires impliquées par les conditions expérimentales (haute vitesse de balayage, t_{ads} courts).

TRAITEMENT DES DONNÉES ET DISCUSSION

Dans la littérature, différents modèles d'adsorption sont admis pour analyser le phénomène d'adsorption, mais les modèles Langmuir [12,13] et Temkin [14,15,16] sont le plus souvent adoptés.

Cependant, ces modèles conduisent souvent à des conclusions contradictoires. L'origine de ces contradictions est généralement associée à la préhistoire de l'électrode, cet argument n'étant pas le seul facteur affectant le phénomène. Par ailleurs, il nous semble que cette situation ne pourrait pas être élucidée par l'utilsation d'autres modèles d'adsorption, plus complexes, qui compliqueraient le phenomène global. C'est pour cette raison que nous avons essayé d'examiner dans quelle mesure nos résultats expérimentaux peuvent être décrits par les modèles Langmuir et Temkin.

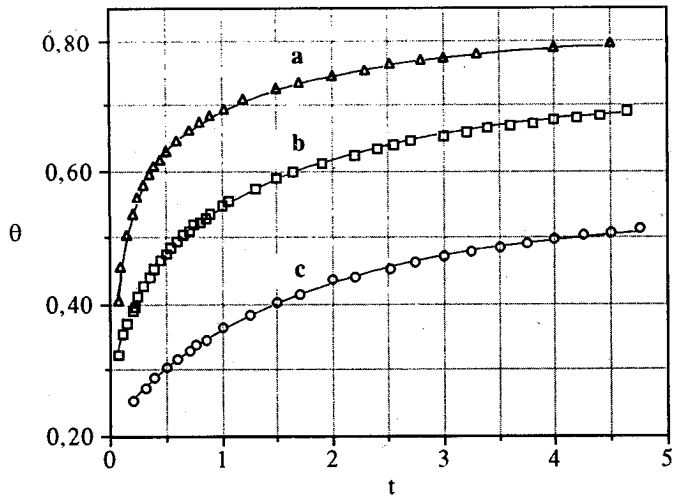

Figure 2. Variation de θ en fonction du temps d'adsorption t à 25°C. (a) C_{MeOH} = 1,0M; (b) C_{MeOH} = 0,1M; (c) C_{MeOH} = 0,01M (0,5M $HClO_4$. E_{ads} = 0,4 V/ERH).

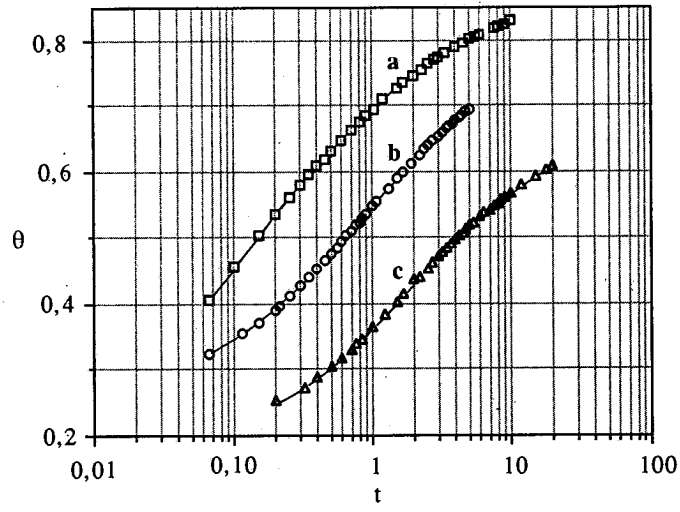

Figure 3. Isothermes cinétiques d'adsorption du MeOH sur Pt lisse à E_{ads} = 0,4 V/ERH. (a) C_{MeOH} = 1,0M; (b) C_{MeOH} = 0,1M; (c) C_{MeOH} = 0,01M.

L'étude a été effectuée aux concentrations 0,01M, 0,1M et 1M en MeOH où les courbes correspondantes θ = f(t) presentent une forme typique (fig.2). Par ailleurs, les diagrammes de la figure 3 montrent que la relation 2 est insuffisante pour décrire le phénomène global. Il est à noter que tous les calculs de θ sont réalisés en considerant le

pourcentage de la surface couvert, par les espèces adsorbées, par rapport à la surface disponible, $\theta = s_{couvert}/s_{disp}$ (s_{disp} = surface accesive à l'adsorption de l'hydrogène). Les détails de ces déterminations ont été déjà décrits [11].

Tout d'abord, nous présentons en détail l'étude d'adsorption du MeOH à partir des solutions de 0,1M en MeOH.

Modèle de Langmuir

Dans ce modèle, on admet qu'il n'y a pas des interactions entre les espèces adsorbées et tous les sites d'adsorption sont équivalents. La vitesse de la réaction d'adsorption à chaque moment est une fonction de la surface libre de l'électrode et la cinétique d'adsorption se décrit par l'équation:

$$\frac{d\theta}{dt} = k'(1 - \theta)^{\alpha} \qquad (4)$$

et

$$k' = k_o C$$

où C est la concentration du MeOH qui reste pratiquement stable au cours d'une expérience, α le nombre de sites occupés par une molécule du MeOH adsorbée et k_o la constante de vitesse de la réaction d'adsorption quand $\theta \rightarrow 0$.

Dans le but de déterminer le paramètres α et k' de l'équation 4, la courbe expérimentale $\theta = f(t)$ a été ajustée à un polynôme de n degré. Nous avons constaté que pour $\theta < 0,6$ cet ajustement conduit à un polynôme de 6^e degré:

$$\theta = A_0 + A_1 t + A_2 t^2 + \cdots + A_6 t^6 = \sum_{i=0}^{6} A_i t^i . \qquad (5)$$

d'où

$$b = \frac{d\theta}{dt} = A_1 + 2A_2 t + 3A_3 t^2 + \cdots + 6A_6 t^5 = \sum_{i=0}^{6} i A_i t^{i-1} . \qquad (6)$$

En conséquence la relation 4 se transforme:

$$\ln b = \ln\left(\frac{d\theta}{dt}\right) = \ln\left\{\sum_{i=0}^{6} i A_i t^{i-1}\right\} = \ln k' + \alpha \cdot \ln\left\{1 - \sum_{i=0}^{6} A_i t^i\right\} \qquad (7)$$

Les coefficients du polynôme 5 déterminés au moyen de la méthode des moindres carrés sont résumés dans le Tableau 1.

La valeur de $\sigma \approx 5,0 \cdot 10^{-4}$ (σ = écart quadratique moyen entre les valeurs calculées et expérimentalement determinées de θ) montre une excellente aptitude de ce polynôme à représenter les données expérimentales. Le diagramme de la figure 4 représente la variation de lnb en fonction de ln(1-θ) pour $\theta < 0,60$. On constate que cette variation est pratiquement linéaire ($R^2 = 0,999$). A l'aide de ce diagramme nous avons calculées la valeur de α trouvée

égale à 4,46. Il en resulte de cette valeur que chaque espèce adsorbée occupe à peu près quatre sites d' adsorption.

Tableau 1. Valeurs des coefficients du polynôme 5.

θ	A_0	A_1	A_2	A_3	A_4	A_5	A_6
0,3 - 0,6	0,2768	0,8045	-1,4816	1,9552	-1,5378	0,6380	-1,1070
0,5 - 0,7	0,3334	0,3866	-0,2553	0,1053	-0,0251	0,0032	$-1{,}6\cdot10^{-4}$

Cependant, en partant de cette valeur de α, le calcul de k' en fonction de t (à l'aide de la relation 4) ne conduit pas à des valeurs de k' indépendentes du temps. Nous avons ainsi constaté que k' varie sensiblement en fonction du t, un fait qui pourrait être expliqué en admettant que α et k' n'ont aucune signification physique, mais au contraire ils sont deux paramètres ajustables. On est ainsi aménè à la conclusion que le modèle de Langmuir ne peut pas représenter l'adsorption du MeOH sur Pt lisse. C'est pourquoi nous avons decidé d'examiner ces phénomènes d'adsorption en nous servant le modèle Temkin, modèle connu pour être efficace dans le cas d'adsorption des molécules simples organiques sur des électrodes de Pt [5,16,18].

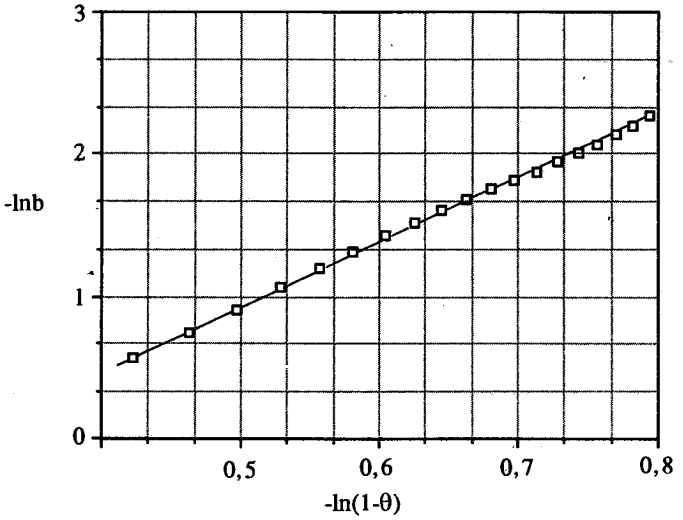

Figure 4. Variation de ln(dθ/dt) en fonction de ln(1-θ). C_{MeOH} = 0,1M

Modèle de Temkin.

Dans ce modèle, on suppose que la surface d'adsorption est uniformement inhomogène, tandis que la variation de ΔG^{o}_{ads} en fonction de θ soit linéaire [19]:

$$\Delta G^{o}_{ads}(\theta) = \Delta G^{o}_{ads}(0) + r\theta$$

On considère aussi que la vitesse d'adsorption depend de la concentration C du MeOH, de la surface libre (1-θ) et d'un facteur exponentiel exp(-gθ) qui est lié a l'inhomogeneité de la surface. L'équation cinétique est:

$$\frac{d\theta}{dt} = k'(1-\theta)\exp(-g\theta) \qquad (8)$$

f étant le facteur de l'hétérogéneité de la surface, α le facteur de symétrie, g = αf et k' = k_0C.

L'équation 3 constitue une forme simplifiée de l'équation 8 et elle se déduit facilement de celle-ci si on admet que (1-θ) varie très peu dans la région $0,2 < \theta < 0,8$.

En tenat compte que la courbe expérimentale θ = f(t) peut être exprimée par un polynôme de n^e degré, la relation 8 prend la forme:

$$\ln Y = \ln k' - g\theta \qquad (9)$$

où

$$Y = \frac{\frac{d\theta}{dt}}{1-\theta} = \frac{\sum_{i=0}^{n} iA_i t^{i-1}}{1 - \sum_{i=0}^{n} A_i t^{i}} \qquad (10)$$

Dans le Tableau 2, nous avons confronté les valeurs expérimentales du degré de recouvrement θ avec celles interpolées à partir de la courbe expérimentale θ = f(t) en utilisant la méthode d'interpolation de Lagrange.

Au but d'examiner dans quelle mesure l'équation 9 est valable dans toute la gamme de θ examinée dans cette étude, la partie de la courbe θ = f(t) correspondant à $0,5 < \theta < 0,7$ a été aussi ajustée à un polynôme de 6^e degré. Nous avons constaté que ce polynôme représente parfaitement les résultats expérimentaux étant donné que $\sigma = 4,9 \cdot 10^{-4}$. Les valeurs obtenues de ses coefficients A_i sont rapportés dans le Tableau 1.

A l'aide de la relation 9 et des coefficients A_i consignés dans le Tableau 1, nous avons calculé les valeurs de Y en fonction du temps t. La courbe de la figure 5 représente la variation de lnY en fonction de θ. La relation 10 prévoit une dépendance linéaire entre lnY et θ; ce que l'on a observé jusqu'à $\theta \approx 0,5$. Dans cette région, le coefficient de détermination linéaire R^2, étant égale à 0,9994, démontre que l'équation 9 est parfaitement valable. En revanche, pour $\theta > 0,5$ on observe des écarts importants de la linéarité. Il est donc possible

de déterminer les paramètres k' et g de l'équation 8 dans la partie linéaire de la courbe lnY = f(t). Les valeurs de ces paramètres ont été trouvées respectivement égales à 7,74 s^{-1} et 6,32

Tableau 2. Valeurs de θ interpolées et expérimentalement déterminées. C_{MeOH} = 0.1M

t/s	θ	t/s	θ
0,0666	0,324*	1,0666	0,556*
0,1166	0,354*	1,30	0,574
0,15	0,370	1,50	0,590
0,20	0,392	1,65	0,599
0,2166	0,398*	1,90	0,612*
0,25	0,410	2,20	0,626
0,30	0,427	2,40	0,634
0,35	0,440*	2,55	0,640*
0,40	0,454	2,70	0,646
0,45	0,465	3,00	0,655
0,50	0,475	3,20	0,661*
0,55	0,485*	3,40	0,666
0,60	0,494	3,60	0,670
0,65	0,502	3,80	0,674
0,70	0,510	4,00	0,679
0,75	0,518	4,20	0,682
0,80	0,524*	4,40	0,686
0,90	0,536	4,65	0,690
1,00	0,548	5,016	0,695*

* Valeurs expérimentales

Il est à noter que la valeur de g (=6,32) coïncide pratiquement avec celle trouvée par Bagotsky et coll. (g=6,25) [6] et Loucka (g=6,4) [20]. Il est à souligner que la valeur 6,25 proposée par Bagotsky et coll. a été determinée à l'aide des isothermes d'adsorption à l'état d'équilibre. Cependant, les mêmes auteurs ont déterminé g à l'aide des données cinétiques et ils ont trouvé la valeur g = 6,5.

Dans le but d'examiner la variation de k' en fonction de t, dans toute la gamme des temps, les valeurs de k' ont été calculées à l'aide de la relation

$$k' = \frac{\frac{d\theta}{dt}}{1 - \theta} \exp(-g\theta), \qquad (11)$$

en utilisant la valeur g = 6,32. L'évolution de k' en fonction de t est illustrée dans le diagramme de la figure 6. On constate que jusqu'à t ≈ 0,8sec (θ ≈ 0,5), le paramètre k' reste pratiquement constant.

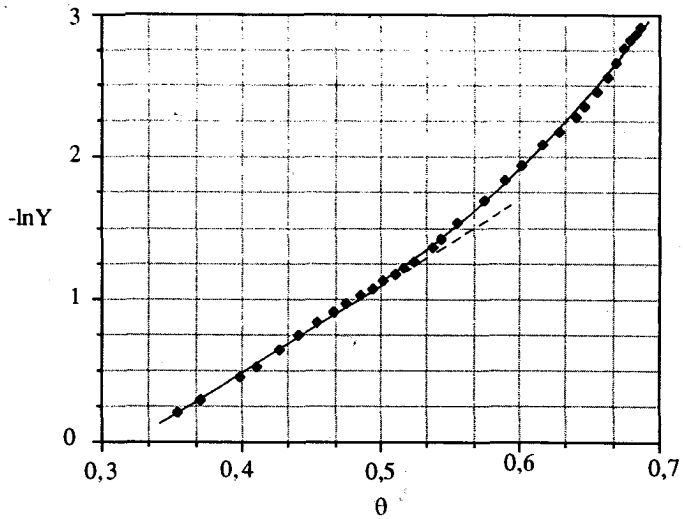

Figure 5. Variation de lnY en fonction de θ. C_{MeOH} = 0,1M

On pourrait interpréter ces résultats si l'on tient compte du fait que l'équation Temkin est une formule limite, rigoureusement valable dans des régions des valeurs relativement faibles de θ, où les interactions entre les espèces adsorbées ne sont pas encore assez importantes.

En outre, il a été postulé dans la littérature [21] que chaque molécule du MeOH, adsorbée sur Pt lisse, occupe deux sites d'adsorption. Étant donnée cette situation, on peut supposer que pour des valeurs θ ≤ 0,5 le phénomène d'adsorption évolue de manière presque idéale sur une surface uniformément hétérogène. Si ceci était vrai, on aurait dû s'attendre à ce que la relation Temkin soit valable jusqu' à θ = 0,5, ce qu'a été effectivement constaté. A partir de θ = 0,5 on peut supposer que des interactions importantes ont lieu entre les espèces adsorbées et le systéme s'écarte sensiblement de la dite allure "Temkin". Quant à la relation cinétique 8, elle perd son aptitude à décrire le phénomène global.

Ces résultats, concernant la concentration 0,1M en MeOH, nous permettent de conclure que pour θ ≤ 0,5 l'équation Temkin s'applique rigoureusement dans le cas du methanol.

En revanche, dans le cas d'une cinétique d'adsorption plus rapide, où θ dépasse rapidement la valeur 0,5, on pourrait supposer que la relation Temkin devient insuffisante pour décrire la situation globale. C'est effectivement ce que nous avons observé dans le cas

où C_{MeOH} = 1,0M. On a constaté que la linéarité prevue par la relation 9 n'est pas observée, même pour de très faibles durées d'adsorption.

Dans le cas où C_{MeOH} = 0,01M, en admetant les dites conditions Temkin, on constate que la dépendance lnY = f(θ) n'est pas linéaire.

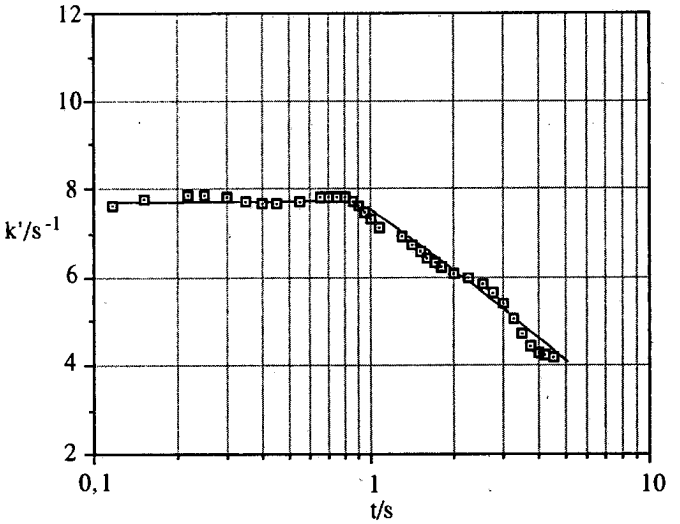

Figure 6. Variation de la constante k' (modéle Temkin) en fonction de t. C_{MeOH} = 0,1M

D'autre part, en examinant les données à l'aide de l'isotherme Langmuir (relation 4) on trouve que, pour differentes valeurs de α, k' ne demeure pas stable en fonction de θ. Cependant, dans les cas où α = 2 ou 3 et θ < 0,3 on constate que k' tend vers des valeurs plus ou moins constantes. Néanmoins, sous de telles conditions (θ < 0,3), la possibilité de réaliser des expériences cinétiques fiables est limitée par la méthode experimentale utilisée dans cette étude.

Conclusions

En conclusion, l'ensemble des calculs effectués et la discussion precédante nous permettent de formuler les remarques suivantes:

L'adsorption du MeOH sur Pt lisse se déroule dans des conditions "Temkin" dans le cas où C_{MeOH} = 0,1M et jusqu'à des valeurs de θ proches de 0,5. Pour θ > 0,5 les interactions entre les molécules "préadsorbées" deviennent plus importantes et par conséquent on observe des écarts par rapport au comportement "Temkin" qui croissent en fonction de θ.

Le fait que les écarts font leur apparition à θ ≈ 0,5 constitue une indication supplémentaire que la molécule du MeOH a besoin deux sites d'adsorption pour qu'elle soit adsorbée.

Dans le cas où C_{MeOH} = 1,0M on ne peut visualiser un domaine de validité de la relation (modèle) de Temkin parce que même pour des témps d'adsorption très courts on arrive à des valeurs de θ égales où plus élevées de 0,5, c'est à dire on arrive très rapidement à l'état de saturation. Dans le cas où C_{MeOH} = 0,01M la situation semble plus compliquée et les deux modèles utilisés sont insuffisants pour décrire le phénomène global. En plus, la concentration 0,01M est considéré assez basse permettant éventuellement l' interventions de divers effets contaminants.

Il est à souligner que les résultats de cette étude sont en accord avec les conclusions d'autres études [6,20]. Les écarts observés entre nos résultats et ces de Wieckowski [23] et Kazarinov [24] peuvent être attribués au fait que ces recherches ont été effectuées sous de conditions sensiblement differentes (adsorption sur Pt platiné).

REMERCIEMENTS

Nous tenons à remercier Monsieur le Professeur C. Lamy, Directeur du Laboratoire *Électrochimie et Interactions* de l'Université de Poitiers et Mr J. M. Léger, Maître de Recherche au CNRS, pour leur aide précieuse lors de la réalisation expérimentale de ce mémoire, ainsi que pour les remarques qu'ils ont bien voulu nous faire.

Summary

KINETIC STUDY OF THE ADSORPTION OF METHANOL ON A SMOOTH POLYCRYSTALLINE Pt ELECTRODE

The kinetic of the adsorption of methanol on a smooth Pt electrode has been studied by using data derived from a programmed cyclic voltammetry technique. The data is treated by means of Langmuir and Temkin equations, the validity of which is discussed. The results obtained show that the Langmuir equation is insufficient to describe the whole phenomenon. On the contrary, Temkin's equation is quite applicable to the solutions where C_{MeOH} = 0,1M. This treatment also shows that both these equations are insufficients to describe the adsorption of methanol from solutions of 1,0 and 0,01M MeOH.

Περίληψη

ΜΕΛΕΤΗ ΤΗΣ ΚΙΝΗΤΙΚΗ ΤΗΣ ΠΡΟΣΡΟΦΗΣΕΩΣ ΤΗΣ ΜΕΘΑΝΟΛΗΣ ΠΑΝΩ ΣΕ ΛΕΙΑ ΠΟΛΥΚΡΥΣΤΑΛΛΙΚΑ ΗΛΕΚΤΡΟΔΙΑ ΛΕΥΚΟΧΡΥΣΟΥ

Στην Εργασία αυτή μελετάται η κινητική της προσροφήσεως της μεθανόλης πάνω σε λεία πολυκρυσταλλικά ηλεκτρόδια Pt. Στη μελέτη αυτή χρησιμοποιούνται πειραματικά δεδομένα που προέκυψαν με τη βοήθεία της τεχνικής της προγραμματιζόμενης κυκλικής βολταμετρίας. Τα δεδομένα αυτά αναλύονται με βάση τα θεωρητικά πρότυπα των Langmuir και Temkin και εξετάζεται η αξιοπιστία των προτύπων αυτών στο να περιγράψουν τα πειραματικά δεδομένα της Εργασίας αυτής. Διαπιστώνεται ότι το

πρότυπο Langmuir σε καμιά περίπτωση δεν μπορεί να περιγράψει το όλο φαινόμενο της προσροφήσεως της μεθανόλης πάνω σε λεία ηλεκτρόδια Pt. Αντίθετα, το πρότυπο Temkin κρίνεται κατάλληλο στο να περιγράψει την πρσρόφηση της μεθανόλης από διαλύματα 0,1M μεθανόλης και για βαθμό επικαλύψεως $\theta < 0,5$. Τέλος διαπιστώνεται ότι οι εξισώσεις Langmuir και Temkin δεν μπορούν να περιγράψουν τα πειραματικά μας δεδομένα όταν $C_{MeOH} = 1,0$ ή 0,01M και $\theta > 0,3$.

Bibliographie

1. B. D. Mc Nicol, *J. Electroanal. Chem.*, **118**,71(1981).
2. M.W. Breiter, *J. Electroc. Soc*, **110**,449(1963).
3. S. S. Beskorovainaya, Yu. B. Vasiliev et V. S. Bagotsky, *Élektrokhimiya*, **2**,167(1965).
4. S. S. Beskorovainaya, Yu. B. Vasiliev et V.S. Bagotsky, *Élektrokhimiya*, **1**,1020(1965).
5. Ya. Yeber, Yu. B. Vasiliev et V. S. Bagotsky, *Élektrokhimiya*, **2**,515, 522(1966).
6. V. S. Bagotsky, Yu. B. Vasiliev, *Electrochimica Acta*, **11**,1439(1966).
7. S. N. Raicheva, E. I. Sokolova et M. V. Christov, *J. Electroanal. Chem.* **175**,167(1984).
8. P. Delahay et D. M. Mohilner, *J. Am. Chem. Soc.*, **84**,4247(1962).
9. P. Nikitas et A. Papoutsis, *Electrochimica Acta*, **33**,683(1988).
10. J. M. Léger, B. Beden et C. Lamy, *Ber. Busenges. Phys. Chem.*, **91**,336(1987).
11. A. Papoutsis, J. M. Léger et C. Lamy, *J. Electroanal. Chem.*, **234**,315(1987).
12. A. Wieckowski et J. Sobkowski, *J. Electroanal. Chem.*, **73**,317(1976).
13. A. Wieckowski, *J. Electroanal. Chem.*, **78**,229(1977).
14. T. Biegler et D. F. A. Koch, *J. Electrochem. Soc.*, **114**,904(1967).
15. E. P. M. Leiva et M. C. Giordano, *J. Electroanal. Chem.*, **158**,115(1983).
16. B. B. Damaskin, O. A. Petrii et V. V. Batrakov, *Adsorption of Organic Compounds on Electrodes*, Plenum Press, 1971.
17. A. A. Mikhailova, N. V. Osestrova et Yu. B. Vasiliev, *Élektrokhimiya*, **15**,1432(1967).
18. V. S. Bagotsky et Yu. B. Vasiliev, *Electrochimica Acta*, **12**,1323(1967).
19. E. Gileadi, *Chemisorption*, p. 11, Plenum Press, New York (1967).
20. T. Loucka, *J. Electroanal. Chem.*, **36**,369(1972).
21. A. M. de Ficquelmont et M. M. de Ficquelmont-Loizos, *J. Electrochem. Soc.*, **131**,2880(1984).
22. H. Angerstein-Kozlowska et B. E. Conway, *J. Electroanal. Chem.*, **95**,1(1979).
23. A. Wiekowski et J. Sobkowski, *J. Electroanal. Chem.*, **63**,365(1975).
24. V. Kazarinov, G. Tysyachnaya et V. Andreev, *J. Electroanal. Chem.*, **65**,391(1975).

Chimika Chronika, New Series, 20, 17-37 (1991)

CATALYTIC PROPERTIES OF γ-Al_2O_3 ELECTROLYTICALLY PREPARED III. EFFECT OF ANODIC OXIDATION BATH TEMPERATURE ON ITS CATALYTIC PROPERTIES

G. PATERMARAKIS

Department of Chemical Engineering, Laboratory of Physical Chemistry and Applied Electrochemistry, National Technical University of Athens, Greece

(Received January 31, 1990)

SUMMARY

The catalytic effect of porous anodic alumina films prepared in H_2SO_4 15% w/v, at constant current density 3.5 A/dm^2, different bath temperatures 20-50°C and anodization time intervals, was investigated in the HCOOH dehydration reaction. For bath temperatures 25, 30 and 40°C it was verified that kinetic parameters such as activation energy, frequency factor, total activity of films having constant geometric surface as well as specific activity displayed a maximum at a particular anodization time interval, for each bath temperature employed, around which the maximum limiting mass, thickness and porosity at first appear. For films prepared at the same anodization time, with identical thickness or pore lenght, all the above parameters increase with increasing bath temperature. The sequence is reversed when their maximum values, except those of specific activity, are compared. Specific activity, on the contrary, increases significantly as bath temperature increases when films having the same thickness values or those displaying maximum values of kinetic parameters are compared. This catalytic behaviour of anodic Al_2O_3 films is partially due to the variation of film porosity which increases with thickness and bath temperature either with regard to films of the same thickness or films with limiting maximum thickness and also to the significant increase of limiting mass, thickness and total real surface of films on decreasing bath temperature. The main reason for the observed catalytic effect of porous anodic aluminas in the HCOOH dehydration is the change in structural characteristics such as the size of microcrystallites and the stoichiometric deviation of the oxide across the compact pore wall Al_2O_3 which are differently affected by bath temperature.

Key words: Catalysis, anodic alumina, formic acid decomposition.

INTRODUCTION

Aluminium oxide films on Al metal surface can be prepared electrolytically by the anodic oxidation of Al metal and are usually called anodic alumina films. These films are of cellular structure and the choise of electrolyte determines the product film: being either non-porous (barrier type), formed in electrolytes which do not dissolve the Al_2O_3 produced (boric acid, borate salts, citric acid etc), or porous, formed in electrolytes dissolving the produced Al_2O_3 (sulfuric, phosphoric, oxalic acids etc)[1,2]. The thickness of non-porous films is approximately analogous to the imposed voltage and can reach up to 1 μm while that of porous ones can reach up to many tens of μm. The structure of porous films is characterized by a close packed array of approximately hexagonal, columnar cells each of which contains an elongated, roughly cyllindrical pore, extending between the film external surface and the Al_2O_3/Al interface where it is sealed by a thin compact barrier type oxide layer. Pore base diameter and cell/pore surface concentration are dependent on the choise of electrolyte. Pore diameter varies generally between a few Å up to a few hundred Å (for H_2SO_4 electrolyte it is equal to or greater than 120 Å) and pore concentration is of the order 10^{10} pores/cm^2 of metal geometric surface.

The investigation of catalytic properties of anodic aluminas has recently acquired much interest. Anodic aluminas either porous or non-porous were applied as planar model or substrate model catalyts and the results appeared to be remarkable[3-14]. The catalytic behaviour of porous anodic alumina films prepared in a 15% w/v H_2SO_4 non-stirred bath solution in the HCOOH decomposition reaction[15-17] was investigated while a semiindustrial catalytic reactor was designed, constructed and studied with respect to the same reference reaction[18]. Formic acid decomposition on these alumina catalysts was found to be a ≃100% dehydration reaction[15,16] up to a temperature of 355°C according to equation

$$HCOOH \longrightarrow H_2O + CO \qquad (1)$$

while the Al metal lying beneath the Al_2O_3 film did not exert any direct influence on the reaction[14].

The activity of the anodic Al_2O_3 catalyst is much higher than that of bulk γ-Al_2O_3 chemically prepared[15]. The HCOOH dehydration reaction was found to be a zero order reaction for HCOOH vapour pressure values greater than a particular one specific for each reaction temperature being i.e. 0.38 and 0.55 at 320 and 350°C[14]. The results suggested a reaction mechanism whereby the HCOOH dehydration takes place on Lewis acidic centers via a formate ion intermediate[14]. The conditions of preparation of anodic aluminas, anodization time and current density, significantly affected the kinetic parameters of HCOOH dehydration i.e. activation energy, frequency factor and both total and specific activities of anodic alumina film catalysts.

In the present study the effect of bath temperature of anodic oxidation on the catalytic properties of anodic aluminas, prepared at constant current density 3.5 A/dm^2 in a 15% w/v H_2SO_4 non-stirred bath solution, in the HCOOH dehydration reaction, was studied.

EXPERIMENTAL

The materials and procedure of Al anodization for the preparation of anodic alumina catalysts, the treatment of anodized Al specimens for the removal of the electrolyte enclosed inside pores and the methods of film mass and thickness determination were reported earlier[16,17]. The Al specimens used were 30x50(mm) coupons with a tailing end the greater portion of which was covered with insulating varnish whereas its bare edge was utilized for making the electrical connection. Prior to anodic oxidation, the Al coupons were cut along the 50 mm horizontal dimension, on either side, into strips 20x2(mm). After anodization, the 20 strips, symmetrically cut around the middle of Al specimen carrying the anodic Al_2O_3 film on the 20.2 cm^2 of their geometric surface, constituted the catalyst supplied to the reactor.

Anodic alumina films prepared at a constant current density, 3.5 A/dm^2, at bath temperatures 20, 25, 30, 40, 45

and 50°C and various anodization time intervals were used as catalysts in HCOOH decomposition experiments. Another group of Al_2O_3 films, prepared at 30°C bath temperature, were calcined at 500°C for about 17 hrs for measuring the weight loss due mainly to the removal of OH groups or molecular H_2O present in the film. The Al_2O_3/Al strips of catalysts prepared at bath temperatures 25–40°C were weighted before and after catalysis experiments, after being dryed in an air stream, in order to determine the total mass change during catalysis due to the amount of H_2O gained or lost and the amount of HCOOH adsorbed on the pore wall surfaces of catalysts. They were subsequently neutralized with NaOH 0.1 N for removing absorbed HCOOH, dried and weighed again for the determination of the absorbed HCOOH.

The HCOOH decomposition experiments were carried out in a Schwab laboratory microreactor[16]. The measurements of reaction rate at different temperatures were obtained in this study as well as previously[16,17] by a dynamic method. The reaction temperature was supplied by means of an oven[16] which was regulated to increase the temperature approximately linearly from ambient temperature up to 290°C at a rate of ≃10°C/min and from 290°C up to 350°C at a rate of 1–2°C/min. The method of reaction rate measurements, during catalysis experiments, was as previously described[16].

RESULTS

1.Structure of the anodic alumina films

The mean thickness (h) and mass (m) of the film present on the 20.2 cm^2 anodized geometric surface of the 20 strips of Al_2O_3/Al catalyst prepared at bath temperatures (b.t.) 25, 30 and 40°C and at constant current density 3.5 A/dm^2 vary with anodization time (t) as shown in Figs 1(a and b). The thickness increases linearly up to a particular anodization time interval (t_1) for each b.t. employed; then the rate of thickness increase slows down up to another, also particular for each b.t., anodization time ($t_=$) where it becomes zero. Beyond $t_=$ the thickness remains constant. The density of compact anodic Al_2O_3 oxide calculated from Faraday's law and the constant rate of thickness growth which is independent of

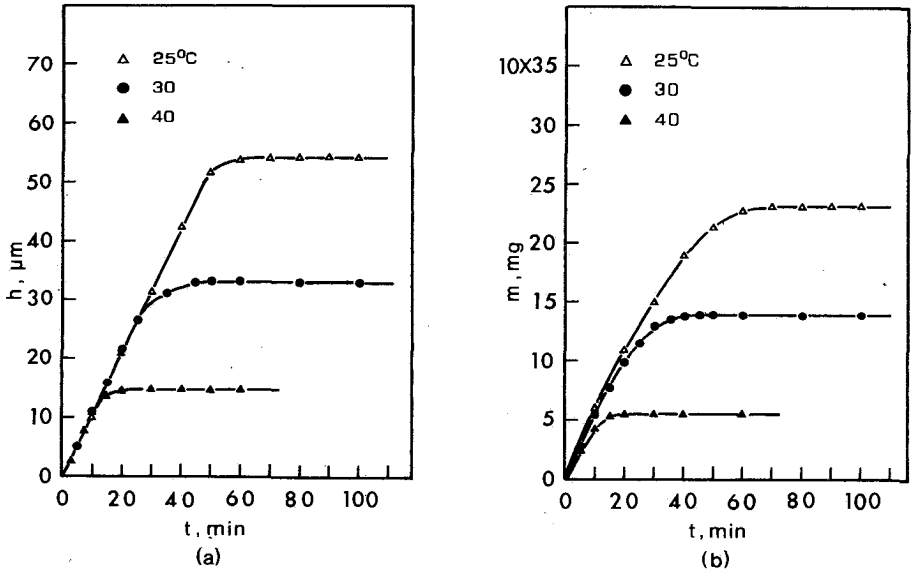

FIG. 1. *Dependence of the mean thickness (a) and mass of the oxide film spread over the 20.2 cm² anodized geometric surface of the 20 strips of Al_2O_3/Al catalyst (b) on anodization time at bath temperatures 25, 30 and 40°C and current density 3.5 A/dm².*

b.t. and anodization time up to t_1 was found to be 3.42 g/cm³. Film porosity values were calculated from the mass, thickness and density of compact Al_2O_3 and were found to increase up to t_c from which point onwards they also remain constant. Since pore concentration remains constant during anodization and pore length is identical to film thickness, the variation of specific real surface with anodization time ought to be qualitatively the same to that of porosity. All these observed facts can be explained on the basis of the close packed array of the approximately hexagonal columnar cell structure of porous films. Figure 2 depicts two sections of an idealized cell, parallel (a) and perpendicular (b) to the direction of thickness growth or pore axis in which the barrier layer, porous layer, pore wall Al_2O_3 and pore and cell shape are also pictured. Because of the internal dissolution of pore walls, during anodization by the electrolyte, pores acquire a conical

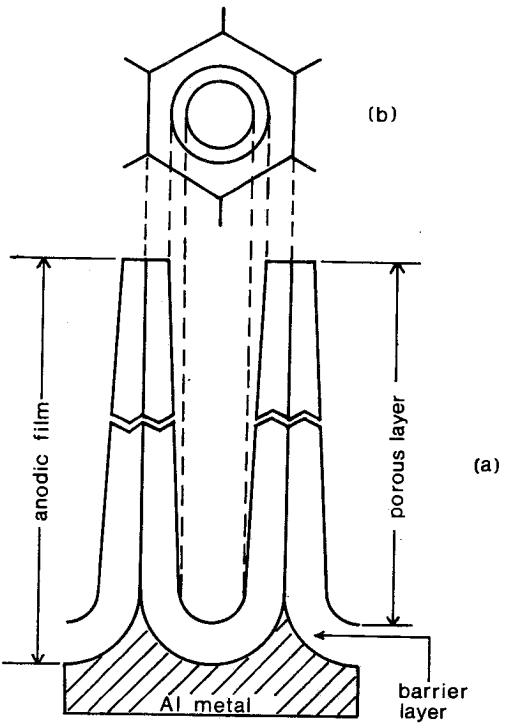

FIG. 2. *Sections of an idealized hexagonal columnar cell of a porous anodic alumina film, parallel (a) and perpendicular (b) to the axis of a truncated cone-shaped pore.*

shape. The linear increase of film thickness up to t_i is justified by the fact that the pore external diameter is smaller than cell width. At t_i the pore diameter approaches cell width while at t_∞ their sizes become equal after which point onwards a constant film thickness is achieved. The changing rate of film thickness growth between t_i and t_∞ is due to the fact that the cross sectional shape of cells is not strictly hexagonal and that, during anodization, some small temperature gradient along the vertical dimension of the Al specimens is established; the temperature is somewhat higher than the imposed b.t. and increases from the lower to the upper regions of the specimen. This results in a local current

density and local film thickness distribution along this direction which becomes significant only when b.t. decreases and current density increases considerably. The thickness of the upper regions of films prepared at anodization times $t<t_1$ was slightly higher than the corresponding thickness of the lower film regions. During the interval t_1-t_∞ this sequence was gradually inversed and this trend persisted even beyond t_∞. The limits, on either side of the mean thickness (film thickness at the middle of the specimen) between which film thickness falls were ±0.5, ±1.5 and ±2.5μm for b.t. 40, 30 and 25°C respectively for $t>t_\infty$ where the deviation of either specimen edge from the mean film thickness was always the largest.

Together with the above mentioned reasons, the process of internal pore wall dissolution explains the continuously decreasing rate of mass growth up to t_∞, the constant mass for anodization times beyond t_∞ and the profile of porosity variation with anodization time. The mechanism of film growth and the simultaneous dissolution of pore wall Al_2O_3 which is enhanced by b.t. also explain the strong depression in the maximum limiting values of mass and thickness with b.t.. The limiting mass of films formed over the 20.2 cm^2 anodized geometric surface of the 20 Al_2O_3/Al strips of catalyst prepared at 20, 45 and 50°C was also determined. It was found to be 0.362, 0.0312 and 0.0213 gr respectively also strongly decreasing with b.t..

The porosity of films having the same thickness and produced at the same anodization time, increases with increasing b.t. but this increase is nevertheless not very significant since pore concentration depends rather on current density. The only reason producing increases in porosity is the larger broadening of pores due to the higher pore wall dissolution capacity when b.t. rises. The porosity of films either when their thickness tends to zero or to the limiting maximum value rises slightly with b.t. varying from 20 up to 28% and from 37 up to 47% respectively on passing from 25 to 40°C. The specific real surface (s) was earlier reported[17] to increase with anodization time from approximately 10 up to 20

m^2/g corresponding to film thickness tending to zero and to its limiting value respectively for films prepared at 30°C and 3.5 A/dm^2. For films prepared at the same b.t. and current densities 1.5-7.5 A/dm^2, although their limiting thickness increases significantly with current density, only a slight increase of limiting s value was verified on decreasing current density[17]. On the basis of what was discussed above for porosity variation the change in specific real surface of films prepared at other b.t. should also vary approximately between 10 and 20 m^2/gr with anodization time although some gentle increase in those values is expected on increasing bath temperature.

The Al_2O_3 anodically produced is a dry material since its calcination showed an insignificant weight loss i.e. 1-2.5% of mass for films prepared at 30°C. These %ages refer to the lower and higher thickness obtained at that b.t. and increased simultaneously with film porosity, denoting that water is adsorbed on the pore surface rather than incorporated in the compact pore wall Al_2O_3. A %age less than unity thus can be regarded as H_2O incorporated in pore wall compact oxide. The above percentages of H_2O contained in the oxide increase slightly with bath temperature.

2.Catalytic decomposition of HCOOH on anodic Al_2O_3 films

Since HCOOH decomposition is an exclussively dehydration reaction of zero order under the experimental conditions of 1 atm HCOOH vapour pressure[16], then the measured reaction rate (r in mol/s) was identical to the reaction rate constant (k). From its values measured at various reaction temperatures and the application of the Arrhenius equation

$$k = A\exp(-E/RT) \quad (1)$$

or

$$\ln k = \ln A - E/RT \quad (2)$$

where E=activation energy in kJ/mol, A=frequency factor in mol/s, R=universal gas constant and T=reaction temperature in K, the E and A values were determined by regression analysis.

The variation of activation energy, frequency factor and

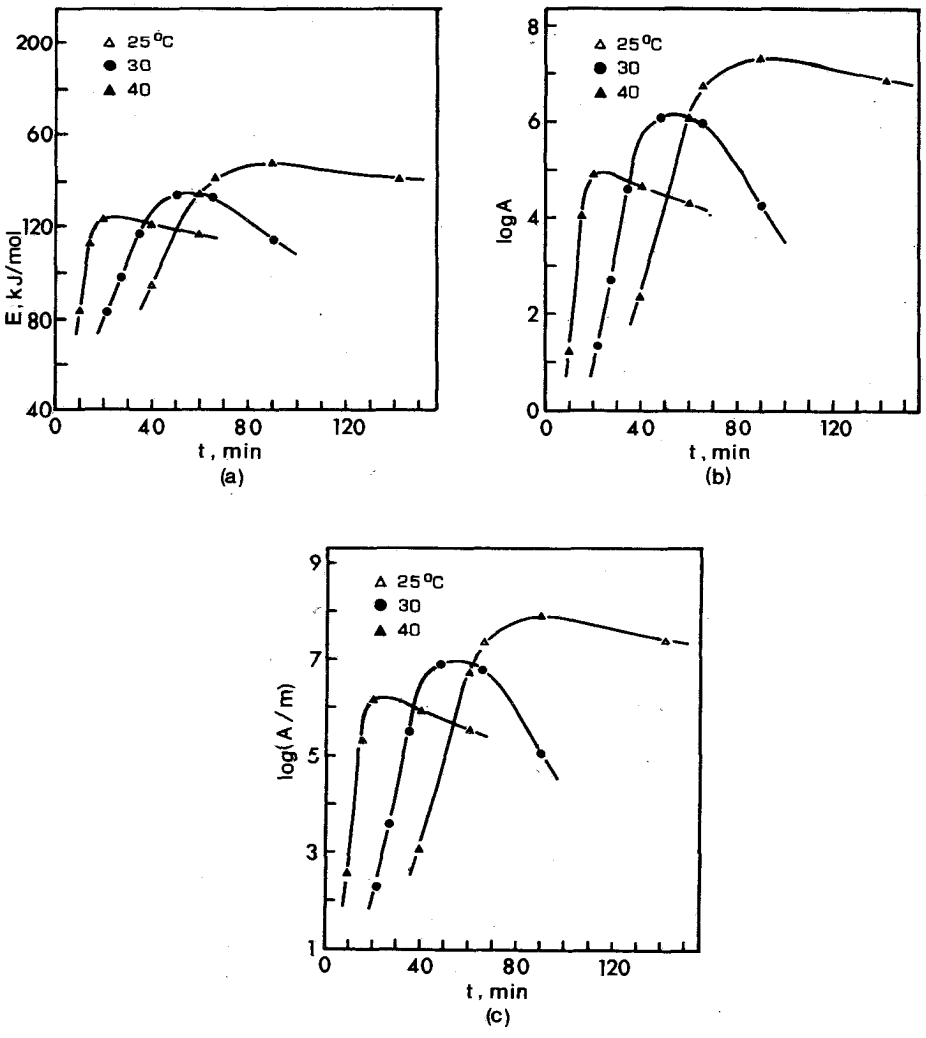

Fig. 3. *Effect of anodic oxidation time on the activation energy (a), frequency factor (b) and reduced frequency factor per gram of oxide (c) displayed by the HCOOH catalytic dehydration of oxide (c) displayed by the HCOOH catalytic dehydration reaction on porous anodic Al_2O_3 films prepared at 25, 30 and 40°C bath temperatures.*

reduced frequency factor per gram of Al_2O_3 film catalyst (A/m in mol/s·g) with anodization time, yielded by the films prepared at 25, 30 and 40°C b.t. is shown in Figs 3(a, b and

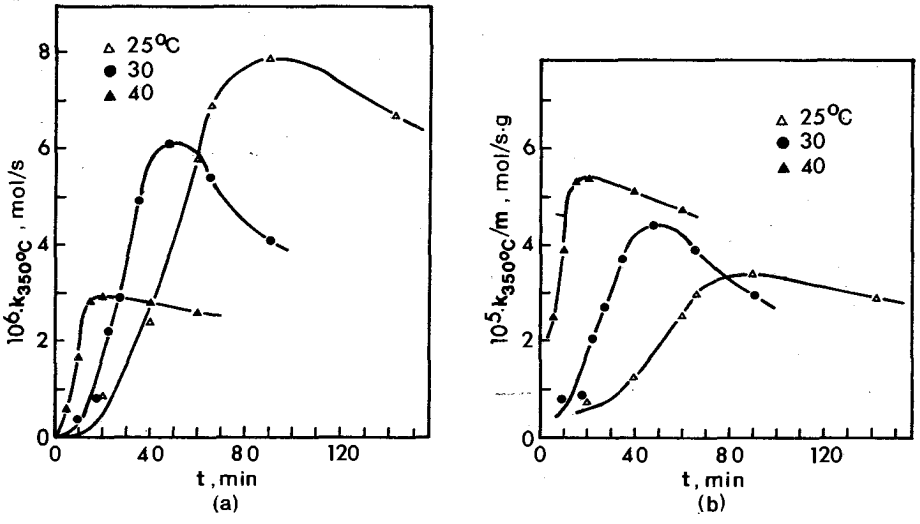

Fig. 4. *Dependence of total activity displayed by the anodic Al_2O_3 present on the 20.2 cm^2 anodized geometric surface of the 20 strips of Al_2O_3/Al catalyst (a) and specific activity (b) at constant reaction temperature 350°C of HCOOH dehydration on anodization time at bath temperatures 25, 30 and 40°C.*

c) respectively. The total activity defined as the activity exhibited by the oxide catalyst suspended on the 20.2 cm^2 anodized geometric surface of the 20 strips of Al metal at a constant reaction temperature of 350°C (k(350°C)) and the specific activity at the same temperature (k(350°C)/m) vary with anodization time at b.t. 25, 30 and 40°C as shown in Figs 4(a and b) respectively. All above kinetic parameters display a maximum around t_m for each b.t. as observed from Figs 3 and 4. This maximum probably vanishes as b.t. becomes >40°C and constant values of kinetic parameters for $t \geq t_m$ are expected. Because of the small value of specific real surface and its unimportant variation with anodization time[17] and b.t. as stated above, the reduced parameters A and k(350°C) per m^2 of real surface (S=m·s) of oxide film (A/S and k(350°C)/S) are expected to have the same profile of dependence with respect to anodization time as A/m and k(350°C)/m while their maximum values must also vary in a similar fashion to that of the A/m

and k(350°C)/m parameters with b.t.. This was also found to be true for films prepared at various current densities at b.t. 30°C[17].

The appearance of maxima in kinetic parameters could be to some extent attributed to the distribution of film thickness and porosity near t_c and about the center of the specimen from which the Al_2O_3/Al strips were taken since the distribution of thickness is probably connected to a distribution of catalyst efficiency also. The inversion of thickness distribution in the interval t_i-t_c which continues at an imperceptible rate and beyond t_c could contribute to the appearance of a maximum in kinetic parameters but since the thickness distribution is noticable only at the lowest b.t. of 25°C the significant variation of kinetic parameters around the maximum observed at i.e. 30°C b.t. cannot be attributed to this reason only. This could probably be the reason for the appearance of maxima not strictly at the anodization time t_c. As it was also previously noted[17], impurities present in the Al metal used for anodic film preparation, such as Fe, do not have any influence on the results; then their presence cannot justify the observed variation in catalytic kinetic parameters.

When films prepared at the same anodization time, having comparable thicknesses which are nevertheless lower than the limiting thickness values, are considered, we observe that all parameters are increasing as b.t. rises. As films approach their limiting thickness, the trend is reversed for all parameters except for specific activity which remains unaltered.

Measurments of kinetic parameters were also taken from experiments of HCOOH decomposition over films prepared at b.t. 20, 45 and 50°C and anodization times 140, 15 and 10 min respectively, corresponding to the time intervals t_c, around which the maximum in kinetic parameters is expected to appear. By comparing the maximum values of kinetic parameters obtained at the different b.t. employed it is observed that the activation energy, frequency factor and reduced frequency factor, Fig. 5(a), and total activity at 350°C reaction

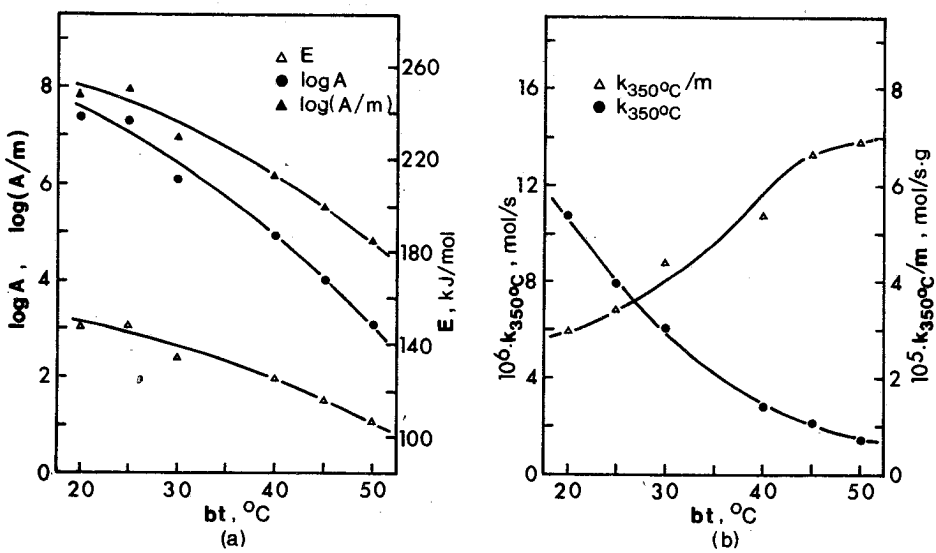

FIG. 5. *Effect of anodic oxidation bath temperature on the maximum values of activation energy, frequency factor and reduced frequency factor per gram of oxide catalyst (a) and total and specific activity at 350°C reaction temperature of HCOOH dehydration (b) achieved at various bath temperatures employed for the preparation of anodic alumina film catalysts.*

temperature, Fig. 5(b), increase with decreasing b.t. whereas specific activity, Fig. 5(b), increases in the reverse direction i.e. with increasing b.t.. The magnitude of maximum specific activity at 50°C is nearly 2.5 times that at 20°C. The increase in specific activity with b.t. is due partially to the increase of porosity and real surface but is mostly due to changes in the nature of pore wall oxide with b.t..

Although the maximum specific activity increases with increasing b.t., the maximum total activity on the other hand increases considerably with decreasing b.t.. It is due to the appreciable increase in the length of pores in films having the maximum limiting thickness as b.t. decreases. Hence the catalytic real surface of pore walls increases significantly, predominating over the decrease in the maximum value of specific activity with decreasing b.t..

Because of the increase in both the pore wall surface due

to the conical shape of pores and the catalytic specific activity of Al_2O_3 with film thickness or pore axis length, the values of parameters E, A/m and k(350°C)/m calculated or those of A/S and k(350°C)/S which represent their mean values over the whole surface of pore walls can be regarded as the values of parameters displayed by a ring-shaped differential of the pore surface, dS, located at an appropriate distance from the pore base and near the pore mouths. Then, the kinetic parameters displayed by this surface must vary with respect to its position along the cross section of pore wall Al_2O_3, Fig. 2, or in other words, the catalytic effectiveness of compact pore wall oxide changes along its section. Thus the observed variation of kinetic parameters with anodization time acquires a physical meaning; it must be attributed to the change of oxide nature along the pore wall section.

The weight of Al_2O_3/Al strip catalysts, prepared at b.t. 25 and 30°C, prior to catalysis, after catalysis and after neutralization was found to be essentially the same. It is therefore concluded that the variations of oxide weight due to the changes in the amount of H_2O lost during experiments and the amount of HCOOH present in the oxide film after catalysis are insignificant; both falling into the limits of weight determination accuracy. Since at ambient temperature increased adsorption of HCOOH is expected, the HCOOH quantity adsorded on the oxide surface during catalysis is therefore also insignificant. This is due to the dissociative adsorption of HCOOH happening only on the small surface of pores and not on the much larger surface of microcrystallites constituting the pore wall oxide[16,17] since it is not accessible to gaseous HCOOH molecules. Water initially present in the film must be to some extent removed by heating during catalysis experiments but since reaction temperature and experimental duration were appreciably lower than that of calcination as noted above, then the H_2O amount removed is lower than that at calcination, which is 1-2.5% for films prepared at 30°C b.t.. This weight loss must be counterbalanced to some extent by adsorption of HCOOH. Weight increases, due to H_2O adsorption during catalysis, must be rather excluded since H_2O produced is

easily removed, a fact arising also from the zero order of reaction. Total weight variation then, after catalysis and catalyst neutralization, is apparently insignificant and hence not accurately measured gravimetrically. Only for Al_2O_3 film catalysts prepared at b.t.≥40°C a weight diminution was observed. After catalysis experiments and the subsequent neutralization of catalysts, weight losses were 1.1 and 1.9% on average respectively for films prepared at 40°C. Their difference of 0.8% is apparently a rough estimation of the amount of HCOOH adsorbed on the catalytic surface after catalysis has ceassed and expresses the HCOOH amount present on saturated pore wall surface. The 1.9% weight loss roughly expresses the water initially present mainly on the pore wall surface. As b.t. increases the film porosity and specific real surface also rise together with the amount of water initially present and the water amount removed during catalysis becomes measurable. The increased amount of HCOOH adsorbed is also due to the increased porosity and specific real surface or to some change of microcrystallite size around the pore wall surface and their surface nature. Probably other incorporated species such as SO_4^{2-} and traces of other element impurities located at the intercrystallite surfaces are reduced on increasing b.t. and the surface around microcrystallites on the pore wall surface becomes more accessible to HCOOH adsorption.

DISCUSSION

A significant diffusion effect of reactant (HCOOH) or products (CO and H_2O) inside pores appearing in the results must be rather excluded when considering the results since: (i) The pore diameter is not extremely narrow (for H_2SO_4 electrolyte the pore base diameter is always equal to or greater than 120 Å). (ii) The pore length is also not very large (thin films) with respect to their diameter. (iii) The conical shape of pores assists reactant and products diffusion inside pores. The decrease in catalytic effectivity of pore wall Al_2O_3 from the cell boundaries to the pore axis direction or, in other words, along the pore wall generative in the direction from the pore mouth to its base, Fig. 2(a), also

contributes to the dissapearance of any noticable diffusion effect. (iv) The activation energy found for all catalysts used in the reaction temperature region examined, 290–350°C, is high suggesting a chemically controlled reaction. Some diffusion effect could be expected in films in which the mean diameter of pores approaches pore base diameter i.e. when film thickness tends to zero. But since the pore length becomes also small the diffusion of reactant and products inside pores is not hindered. Additionally, the high value of activation energy excludes this case. Even in cases of very long pores (thick films prepared at low b.t.), where a narrow pore base diameter and a small inclination of pore wall with respect to pore axis are expected, the part played by diffusion control at the bottom of pores is insignificant and the portion of the total reaction effect controlled by diffusion must be very small and overshadowed by the overall rection effect. The activation energy estimated also suggests a chemically controlled reaction. The increase in maximum activation energy with b.t. diminution constitutes also an indication for the above reasoning.

Hence the variation of kinetic parameters E, A, A/m, k(350°C) and k(350°C)/m with both anodization time and b.t. must be mainly attributed to changes in the nature of compact Al_2O_3 along the pore wall section. Two structural characteristics coexisting were previously recognised as the main factors determining the number and intensity of Lewis acidic centers on which HCOOH dehydration takes place via a formate intermediate and which are responsible for the catalytic effectiveness of porous anodic aluminas. These were the crystallinity of oxide increasing with anodization time and the deviation of oxide from its stoichiometric ratio in favour of oxygen atoms (p-semiconductivity) decreasing with film thickness[14]; according to what has been mentioned earlier in the present study their variation must be viewed with respect to the cross section of the pore wall oxide, Fig. 2(b).

From the mechanism of film production in the hemispherical units of barrier layer at the base of pores, Fig. 2(a), the increase in the surface of ion charge exchange

along the electrolyte/Al_2O_3 interface towards the Al_2O_3/Al interface direction, during anodization, causes a gradient of the true density of ionic current which diminishes along it; hence a similar intensity gradient for these two factors is expected. As the true current density decreases, the "oxygen ion" accumulation and oxygen atom surplus, after anodization has already been completed, decrease along this direction. Additionally, as the ionic current decreases, crystallite size (crystallinity) increases since it is known that, generally, in electrochemical reactions the increase in their rate (current density) causes a diminution in grain size in the solid material produced or deposited. These changes across the barrier layer evidently happen also across the pore wall Al_2O_3 since as anodization proceeds the barrier layer is converted into pore wall Al_2O_3. Crystallinity of pore wall Al_2O_3 could also increase not only across its section but also on average over the whole oxide on progressing anodization. The production of film at the very early stages of anodization, where the surface of charge exchange is the lowest i.e. that of the geometric Al specimen surface (compared to the mean surface of charge exchange across the barrier layer), takes place with the greatest possible true current density and the lowest possible crystallite size is then expected. The size of crystallites initially formed behaves as a matrix for the subsequently produced oxide although the mean surface of ionic charge exchange increases after the ultimate formation of barrier layer and pore base shape. This influence on the crystallite size decays with anodization time; hence anodization time "per se" causes an increase in the average crystallite size.

As anodization proceeds and oxide thickness increases, the internal pore wall oxide dissolution continuously produces new layers of pore wall Al_2O_3 which become new pore wall surface. New ring shaped surfaces, dS, determining catalytic activity also appear having greater crystallite size and lower oxygen surplus. The cooperation of these two factors gives rise to all kinetic parameters and a maximum around anodization time t_m appears as previously described[16]. The

b.t. rise exerts a promotive influence on the process of crystallite final size establishment and this is probably why the maximum in kinetic parameters for b.t.≥40°C almost vanishes.

It was observed in Figs 3 and 4 that parameters E, A, A/m, k(350°C) and k(350°C)/m dispayed by the Al_2O_3 films with identical thicknesses but lower than the limiting ones, prepared at the same anodization time, decrease as b.t. decreases. This is due, generally, to that on decreasing b.t. the pore base diameter decreases while the thickness of both the barrier layer and pore wall oxide increases. The conversion of layers lying at the interior of the bulk of pore wall Al_2O_3, which are more active, into pore wall catalytically effective surface takes place at a lower rate due to the depression in the rate of dissolution of pore walls by electrolyte during anodization. Thicker pore walls formed at lower b.t. also denote that a lower crystallite size as well as higher semiconductivity are established on the pore wall surface of low thickness films. The second factor predominating causes a lowering in E, A, A/m, k(350°C) and k(350°C)/m according to what was previously suggested[14].

With rising b.t. a higher crystallite size and a lower p-semiconductivity are expected denoting that the innermost surface (cell boundaries) exposed by pore wall dissolution at anodization time t_a which determines decisively the total surface catalytic activity, acquires a nature characterized by higher crystallinity and lower p-semiconductivity. Higher crystallinity provides a lower number of Lewis acidic sites of lower intensity and the decrease in the maximum values of activation energy and frequency factor are thus explained. Lower also specific activity would be expected if crystallite size were the only reason. But the coexistence of semiconductivity which decreases with b.t. probably influences the parameters E and A in a different manner or intensity for each one of them. Eventhough some rise of E and A or A/m is expected from a p-semiconductivity decrease, they are also influenced by increases in crystallinity with b.t. while the contributing result from E and A/m variation gives

rise to specific activity. Another reason for the observed change of specific activity with b.t. is probably that the small amount of H_2O absorbed on pore walls or incorporated inside compact Al_2O_3, its quantity increasing with b.t., is removed on heating during catalysis and to a certain extent gives rise to the active surface; this is generated by the partial separation of collapsed microcrystallites on the pore wall surface. A significant increase in activation energy with b.t. would be expected also. As this is not the case it is concluded that this kind of activity promotion is insignificant and thus the observed variation of kinetic parameters in the catalytic dehydration of HCOOH over anodic porous Al_2O_3 is attributed to the change in both the size of crystallites constituting the compact pore wall Al_2O_3 and the p-semiconductivity which vary significantly across the pore wall oxide and are strongly influenced by bath temperature.

CONCLUSIONS

From the results of the present study the following conclusions can be drawn.

1.The catalytic effect of porous anodic alumina films on the HCOOH dehydration reaction at 290-350°C reaction temperatures was found to be strongly influenced by the conditions of Al anodization: bath temperature and anodization time. Kinetic parameters of HCOOH catalytic dehydration such as activation energy, frequency factor, total activity exhibited by films of the same geometric surface as well as specific activity at a constant reaction temperature strongly vary with anodization time and bath temperature.

2.For Al_2O_3/Al catalysts prepared at the same current density, 3.5 A/dm^2, and at bath temperatures 25, 30 and 40°C it was revealed that all the above parameters displayed a maximum around a specific anodization time for each bath temperature; this specific time decreases as bath temperature increases and is that at which maximum values of thickness, mass and porosity are first achieved. The observed maximum of parameters rather disappears at bath temperatures beyond 40°C,

those remaining constant beyond t_{∞}.

3.For the same thickness of Al_2O_3 films at various b.t. produced at the same anodization time, being nevertheless lower than limiting thicknesses, the kinetic parameters were found to increase together with bath temperature. This sequence for all kinetic parameters, except for specific activity, is reversed when films displaying maximum values in kinetic parameters, prepared at 20-50°C bath temperatures, are compared.

4.The specific activity of Al_2O_3 films was found generally to increase significantly with bath temperature either when films of the same thickness produced at the same anodization time or those exhibiting a maximum in kinetic parameter values are compared.

5.Although specific activity increases with bath temperature, the maximum total activity was found to increase strongly in the opposite direction to that of specific activity namely with decreasing bath temperature due to the strong increase in the limiting thickness and catalytically active surface of conical pores.

6.This catalytic behaviour is mainly due to the variation of the two determining factors, crystallite size and deviation of Al_2O_3 from its stoichiometric ratio (oxygen atoms surplus), across the pore wall compact Al_2O_3. Both of them are affected by bath temperature while the part played by each one of them is unequally affected by bath temperature changes with respect to the intensity or manner of their influence on the catalytic effectiveness of the oxide. Other factors such as diffusion of reactant and products inside pores and a small H_2O amount present in the film appeared to have no appreciable effect on the catalytic effectiveness of the porous anodic aluminas used.

ΠΕΡΙΛΗΨΗ

ΚΑΤΑΛΥΤΙΚΕΣ ΙΔΙΟΤΗΤΕΣ ΤΟΥ ΗΛΕΚΤΡΟΛΥΤΙΚΟΥ γ-Al_2O_3.
III.ΕΠΙΔΡΑΣΗ ΤΗΣ ΘΕΡΜΟΚΡΑΣΙΑΣ ΛΟΥΤΡΟΥ ΑΝΟΔΙΚΗΣ ΟΞΕΙΔΩΣΗΣ ΣΤΙΣ ΚΑΤΑΛΥΤΙΚΕΣ ΤΟΥ ΙΔΙΟΤΗΤΕΣ.

Στην εργασία αυτή μελετήθηκαν οι καταλυτικές ιδιότητες

μεμβρανών πορωδών ανοδικών οξειδίων του αργιλίου, που παρασκευάστηκαν σε λουτρό H_2SO_4 15% σε σταθερή πυκνότητα ρεύματος 3.5 A/dm^2 και διάφορες θερμοκρασίες λουτρού 20–50°C κάι χρόνους ανοδικής οξείδωσης, στην καταλυτική αφυδάτωση του μυρμηκικού οξέος, σε εργαστηριακό μικροαντιδραστήρα. Σε θερμοκρασίες λουτρού παρασκευής μεμβρανών πορωδών Al_2O_3 25, 30 και 40°C παρατηρήθηκε ότι οι κινητικές παράμετροι ενέργεια ενεργοποίησης, παράγοντας συχνότητας, ολική δραστικότητα μεμβράνης οξειδίου σταθερής γεωμετρικής επιφάνειας καθώς και η ειδική του δραστικότητα εμφανίζουν μέγιστο γύρω από κάποιο χρόνο ανοδικής οξείδωσης ιδιαίτερο για κάθε θερμοκρασία λουτρού στον οποίο επιτυγχάνεται η μέγιστη δυνατή τιμή του πάχους, της μάζας και του πορώδους των μεμβρανών οξειδίων. Για θερμοκρασίες μεγαλύτερες από 40°C και για χρόνους μεγαλύτερους από αυτούς, σταθερή τιμή των παραμέτρων μάλλον υποστηρίζεται από τα αποτελέσματα της εργασίας αυτής. Σε καταλύτες μεμβράνες πορωδών Al_2O_3 με ίδια πάχη ή με ίδιο μήκος πόρων που παράγονται στον ίδιο χρόνο ανοδίωσης, που είναι ωστόσο μικρότερα από τα οριακά επιτυγχανόμενα πάχη, όλες οι παραπάνω παράμετροι αυξάνονται με την αύξηση της θερμοκρασίας λουτρού. Η εξάρτηση όλων των κινητικών παραμέτρων εχτός της ειδικής δραστικότητας από τη θερμοκρασία λουτρού αντιστρέφεται όταν συγκριθούν οι μέγιστες επιτυγχανόμενες τιμές τους. Η ειδική δραστικότητα αντίθετα, αυξάνει με τη θερμοκρασία λουτρού και όσον αφορά μεμβράνες Al_2O_3 που έχουν το ίδιο πάχος για ίδιο χρόνο ανοδίωσης και όσον αφορά αυτές που εμφανίζουν τις μέγιστες τιμές στις κινητικές παράμετρες. Αυτή η καταλυτική συμπεριφορά του ανοδικού Al_2O_3 στην αφυδάτωση του HCOOH μερικά μόνο ερμηνεύεται από τη μεταβολή του πορώδους που αυξάνεται με το πάχος του οξειδίου αφού οι πόροι είναι κωνικού σχήματος καθώς και με τη θερμοκρασία λουτρού και για οξείδια με ίδιο πάχος για ίδιο χρόνο ανοδίωσης και γι'αυτά με το μέγιστο δυνατό πάχος. Ο κυριώτερος λόγος για τη μεταβολή αυτή των καταλυτικών παραμέτρων είναι η μεταβολή δομικών χαραχτηριστικών όπως το μέγεθος των μικροκρυσταλλιτών από τους οποίους αποτελείται το συμπαγές Al_2O_3 της μεμβράνης και η εκτροπή από τη στοιχειομετρική αναλογία του οξειδίου με περίσσεια ατόμων οξυγόνου (p–ημιαγωγιμότητα) κατά μήκος της τομής του συμπαγούς Al_2O_3 που αποτελεί τα τοιχώματα των πόρων. Ο διαφορετικός τρόπος με τον οποίο η θερμοκρασία λουτρού επιδρά σε καθ' ένα από αυτούς τους παράγοντες είναι υπεύθυνος για την εξάρτηση των κινητικών παραμέτρων της καταλυτικής διάσπασης του HCOOH από την θερμοκρασία λουτρού παρασκευής των οξειδίων καταλυτών. Η σημαντική αύξηση της μέγιστης ολικής δραστικότητας του ανοδικού Al_2O_3 με τη μείωση της θερμοκρασίας λουτρού, που είναι αντίθετη με την εξάρτηση της ειδικής δραστικότητας από τη θερμοκρασία λουτρού, οφείλεται στη μεγάλη αύξηση του οριακού πάχους της μεμβράνης Al_2O_3 και στη μεγάλη αύξηση επομένως της πραγματικής, καταλυτικά δραστικής επιφάνειας που υπερισχύει έναντι της μείωσης της ειδικής δραστικότητας με την μείωση της θερμοκρασίας λουτρού.

REFERENCES

1. Young, L. :*Anodic Oxide Films*, pp. 193-221, Academic Press, London (1961).
2. Diggle, J., Downie, T. and Coulding, C. :*Chem. Rev.*, **69**, 365 (1969).
3. Cocke, D., Johnson, E. and Merill, R. :*Catal. Rev.-Sci. Eng.*, **26(2)**, 163 (1984).
4. Ruckenstein, E. and Malhotra, M. :*J. Catal.*, **41**, 303 (1976).
5. Chu, Y. and Ruckenstein, E. :*Ibid.* **55**, 281 (1978).
6. Chen, J. and Ruckenstein, E. :*Ibid.* **69**, 254 (1981).
7. Rai, K. and Ruckenstein, E. :*Ibid.* **40**, 117 (1975).
8. Chu, Y. and Ruckenstein, E. :*Ibid.* **41**, 384 (1976).
9. Honicke, D. :*Appl. Catal.*, **5**, 197 (1983).
10. Honicke, D. :*Ibid.*, **5**, 199 (1983).
11. Glassl, H., Kramer, R. and Hayek, K. :*J. Catal.*, **63**, 167 (1980).
12. Glassl, H., Kramer, R. and Hayek, K. :*Ibid.*, **68**, 388 (1981).
13. Glassl, H., Hayek, K. and Kramer, R. :*Ibid.*, **68**, 397 (1981).
14. Glassl, H., and Hayek, K. :*Thin Solid Films*, **89**, 413 (1982).
15. Skoulikidis, Th. and Sarropoulos, C. :*Proc. ICSOBA, 4th, Athens*, Vol. 3, pp. 356-374 (1978).
16. Patermarakis, G. :*Chimika Chronika (N.S.)*, **16**, 141 (1987).
17. Patermarakis, G. : *Ibid*, **18**, 115 (1989).
18. Skoulikidis, Th. and Patermarakis, G. :*Aluminium*, **65**, 185 (1989).
19. Baker, B. and Pearson, R. :*J. Electrochem. Soc.*, **119**, 160 (1972).

Chimika Chronika, New Series, 20, 39-49 (1991)

REVIEW

UNPERTURBED DIMENSIONS AND TEMPERATURE COEFFICIENTS OF POLYMETHACRYLATES WITH HYDROCARBON SIDE GROUPS*

N. HADJICHRISTIDIS

Department of Chemistry
University of Athens, Panepistimiopolis
Zografou, Athens (15771) Greece

Z.XU

Department of Polymer Science and Eng.
East China University of Chemical Technology
Shanghai 200237, People's Republic of China

J. W. MAYS

Department of Chemistry
University of Alabama at Birmingham
Birmingham, Alabama 35294 USA

(Received February 11, 1991)

ABSTRACT

The unperturbed dimensions of polymethacrylates with hydrocarbon side groups have been reviewed in order to elucidate the effects of the nature of the side group on the unperturbed posture of the chain. Unperturbed dimensions of these polymers are influenced not only by the size and rigidity of the substituent, but also by its proximity to the backbone. Unperturbed chain dimensions are also influenced appreciably by tacticity, solvent environment, and, in some cases, temperature.

Key words: polymethacrylates, microstructure,unperturbed dimensions, characteristic ratio, solvent and temperature effects.

INTRODUCTION

Polymethacrylates are one of the most important classes of synthetic polymers.Apart from their most common application, namely poly(methyl methacrylates)'s (PMMA) use as a "glass substitute", many more "high-technology" applications such as their use in biomedical work (1,2) and as polymer side-chain liquid crystals (3,4) have evolved.

The prime reason for the diversity of applications for these materials is the ease with which the physical and chemical properties can be manipulated simply by changing the nature of the ester substituent. Fine-tuning of properties is also allowed by controlling parameters such as tacticity, molecular weight, and branching.

In attempting to correlate (and ultimately predict) properties of polymethacrylates as a function of side group structure, a knowledge of variation of unperturbed chain dimensions with chemical structure is essential. Unperturbed dimensions are the characteristic average dimensions exhibited by the macromolecule in the bulk amorphous state. Thus, such dimensions are readily measured in bulk via neutron scattering experiments involving isotopically (deuterium) labelled chains. Unperturbed dimensions are, for practical reasons, much more commonly measured in dilute solution, usually at the Flory theta (Θ) condition (5). The two primary means for measuring macromolecular size are light scattering and intrinsic viscosity [η] measurments. At the Θ state, the former measures directly the unperturbed mean-square radius of gyration $\langle s^2 \rangle_0$; the latter technique yields the unperturbed parameter K_Θ assuming molecular weight (M) is known (6,7)

$$K_\Theta = [\eta]_\Theta / M^{1/2} \qquad (1)$$

The unperturbed mean-square end-to-end distance $\langle r^2 \rangle_0$ is calculated by (6,7)

$$K_\Theta = \Phi_0 (\langle r^2 \rangle_0 / M)^{3/2} \qquad (2)$$

where Φ_0 is a hydrodynamic constant ($2,5 \times 10^{21}$ (5,8,9)).
From $\langle r^2 \rangle_0$ the characteristic ratio C_∞ can be determined (10,11)

$$C_\infty = \lim_{n \to \infty} \langle r^2 \rangle_0 / nl^2 \qquad (3)$$

where n is the number of main chain bonds of average length l. Since $\langle r^2 \rangle_0 = 6 \langle S^2 \rangle_0$, C_∞ is also directly obtained from a light scattering experiment. Extrapolation procedures are available which allow an estimation of unperturbed dimensions to be made using light scattering or $[\eta]$ data obtained in thermodynamically good solvents (12-15).

An examination of equation 3 indicates that the characteristic ratio is a measure of departure of real polymer chains from the hypothetical limit of greatest flexibility: a freely-jointed chain where $\langle r^2 \rangle_0 = nl^2$ and $C_\infty = 1$. Thus, real polymer chains will exhibit C_∞ values larger than 1, with larger values corresponding to less flexible chains.

Since C_∞ reflects chain dimensions in the bulk amorphous state, it is not surprising that a number of fundamental polymer properties of practical value such as the glass transition temperature (T_g) (16) and the elastic modulus (G) depend directly on C_∞ (17). In the present review, we correlate C_∞ with the structure of the side group for polymethacrylates having hydrocarbon substituents. The influences of the size, flexibility, and distance of the center of mass of the substituent from the backbone are established. We also tabulate the results available on the temperature dependence of C_∞ and comment briefly on the effects of tacticity and the chemical nature of the Θ solvent.

TABULATION AND DISCUSSION OF C_∞ RESULTS

In Table I we present the results for C_∞ of 30 different polymethacrylates having aliphatic, alicyclic and aromatic substituents. Every effort was made to exclude data which appear to be anomalous, and, where several data sets were available, we have tried to choose the most reliable results using criteria such as polydispersity, use of absolute

molecular weights, measurement directly in a Θ solvent, etc. Also, the data are restricted to results obtained on products of free radical polymerization.

TABLE I: Tabulation of C_∞ Results

Substituent	Solvent	Temperature (°C)	C_∞	Ref(s)
methyl	4-heptanone	33.8	7.3	18,19
ethyl	isopropanol	36.9	8.2	20
n-butyl	isopropanol	23.7	8.6	21
n-hexyl	isopropanol	32.6	11.1	22
n-decyl	ethylacetate	11.0	13.4	23
n-dodecyl	n-amylalcohol	29.5	14.5	24,25
n-tridecyl	ethylacetate	27.0	14.9	23
n-octadecyl	n-propylacetate	36.0	20.6	23
n-docosyl	amylacetate	31.0	24.1	23
tert-butyl	cyclohexane	10.0	10.2	26
2-ethylbutyl	isopropanol	27.4	9.8	27
cyclobutyl	n-butanol	37.5	10.0	28
cyclopentyl	cyclohexane	36.0	10.9	28
cyclohexyl	n-butanol	23.0	11.6	29
cyclooctyl	s-butanol	45.0	11.9	28
cyclododecyl	n-hexylacetate	35.0	14.2	28
2-decahydronaphthyl	dipropylketone	25.0	14.8	30
isobornyl	1-octanol	36.9	12.3	31
5-p-menthyl	methylpropylketone	25.0	15.4	32
4-tert-butylcyclohexyl	n-butanol	25.0	12.0	33,34
phenyl	acetone	25.0	13.5	29
benzyl	cyclopentanol	73.2	9.0	35
diphenylmethyl	3-heptanone	45.0	14.0	36
triphenylmethyl	hexamethylphosphoric triamide	25.0	20.3	37
2-tert-butylphenyl	cyclohexane	18.4	12.8	32
4-tert-butylphenyl	cyclohexane	25.0	14.6	34
β-naphthyl	benzene	25.0	16.9	30
4-biphenyl	benzene	25.0	16.4	38
2-biphenyl	1,4-dioxane	25.0	17.8	39
4-(1,1,3,3-tetra-methylbutylphenyl)	benzylacetate	14.0	18.7	40

Ignoring the impact of temperature, tacticity, and the chemical nature of the Θ solvent (these effects are discussed below), we can conclude from the results of Table I that C_∞ increases with: 1) an increase in the size of the substituent, 2) an increase in stiffness of the substituent, and 3)

closer center of mass of the substituent to the polymer main-chain (backbone). In general, anything which restricts rotation about backbone bonds will increase C_∞. Some examples are discussed below.

The effect of size is easily observed in both the n-alkyl series and the alicyclic series. In both cases, a steady increase of C_∞ is seen with an increase in the number of carbons in the side group. Similarly, the effects of substituent size are seen on comparing benzyl (C_∞ =9.0) to diphenylmethyl (C_∞ =14.0) to triphenylmethyl (C_∞ =20.3) substituents.

The effect of flexibility of the side group is evident on comparing the C_∞ values of n-alkyl methacrylates with those of their alicyclic analogues with the same number of carbons. For small ring sizes, where the ring is relatively rigid, C_∞ is larger than that of the corresponding n-alkyl polymer. For larger ring sizes, where the ring is more flexible, C_∞ values are essentially the same. Also, C_∞ is larger for poly(phenyl methacrylate) (C_∞ =13.5) than for poly(cyclohexyl methacrylate) (C_∞ =11.6), due primarily to the stiffness of the phenyl ring. In this last case, specific interactions between aromatic groups may also contribute to the observed difference.

An interesting example where the relative importance of size versus flexibility may be compared is shown below. For poly(isobornyl methacrylate) (PIBM) and poly(5-p-menthyl methacrylate) (PMM).

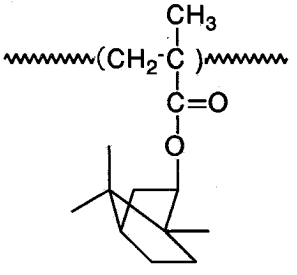

PIBM C_∞=12.3

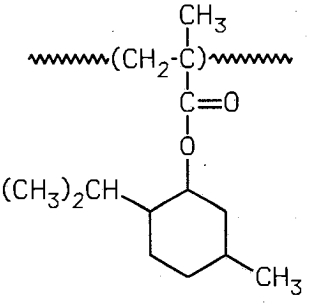

PMM C_∞=15.4

PIBM contains the relatively rigid bridged ring, but PMM has the larger C_∞ because of its larger size.

The effect of the closeness of the center of mass to the backbone is evident on comparing 2-biphenyl (P2BM) and 4-biphenyl(P4BM) substituents:

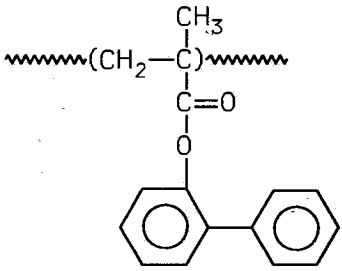

P2BM C_∞ = 17.8

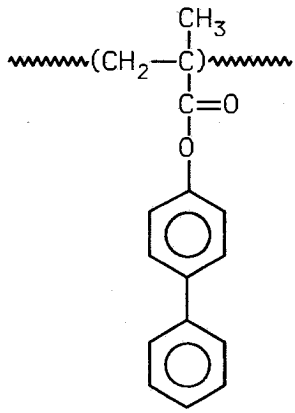

P4BM C_∞ = 16.4

Although the side groups are identical, attachment in the 2-position brings the center of mass closer to the backbone and introduces larger hindrances to backbone rotation. Similarly, poly(benzyl methacrylate) has a much lower C_∞ than poly(phenyl methacrylate), despite its larger size, for the same reason.

In our comparison thus far, we have ignored temperature effects on C_∞. Both theory and experiment (10) indicate, however, that for most chains such effects are of significance, if measurements are conducted at temperatures which differ greatly. Fortunately, most of the results summarized in Table I were conducted near room temperature.

Experience has shown that $\ln C_\infty$ varies approximately linear with temperature. Both negative and positive values of $d\ln C_\infty/dT$ have been observed; the former values result when more compact chain postures are of higher energy, while in the latter case the more compact configurations are of lower energy (10). Temperature coefficients for a number of polymers have been reviewed by Mark (41). Methods for measuring $d\ln C_\infty/dT$ include the stress-temperature (ST) technique, derived from rubber elasticity theory, and measurement of intrinsic

viscosities in a series of theta solvents (VT). Temperature coefficients for free radically produced polymers with hydrocarbon side groups are presented in Table II.

TABLE II: Temperature Dependence of the Characteristic Ratio for Polymethacrylates with Hydrocarbon Substituents.

Substituent	$d\ln C_\infty/dT \times 10^3$	Method	Ref.
methyl	1.6	VT	18
isopropyl	2.5	ST	42
n-butyl	2.5	ST	42
n-butyl	2.3	VT	43
s-butyl	-0.2	ST	42
isobutyl	0.05	ST	44
t-butyl	0	VT	26
isopentyl	1.4	ST	42
n-hexyl	2.2	ST	42
n-octyl	2.2	ST	42
n-dodecyl	2.6	ST	42

C_∞ is observed to be rather large and positive for the n-alkyl derivatives.The value reported in Table II for PMMA is in good agreement with theoretical values calculated via the rotational isomeric state (RIS) approach for predominantly syndiotactic PMMA (45,46). RIS models have not yet appeared for other polymethacrylates. Good agreement between $d\ln C_\infty/dT$ values obtained by the ST and VT methods are noted for poly(n-butyl methacrylate) (42,43). Introduction of branching into the side chain in the case of butyl derivatives leads to a substantial change in $d\ln C_\infty/dT$, from large and positive to essentially zero for the t-butyl polymers. Branching changes the shapes (steric requirements) of these substituents, resulting in substantially different relative energies for their rotational isomers.

As mentioned above, tacticity can also have an effect on C_∞. This is not surprising since the impact of tacticity on morphology and other properties has been documented for many years. Polymethacrylates prepared by free radical polymerization are predominantly syndiotactic.

PMMA samples of varying tacticity have been studied by Jenkins and Porter (47,48). C_∞ values increase from about 7 for highly syndiotactic PMMA to about 10 for highly isotactic samples. It should also be noted that RIS models (47,48) predict a negative temperature coefficient for isotactic PMMA, in agreement with experiment (49). This is, of course, a markedly different result than the positive value cited above (Table III) for highly syndiotactic PMMA. Also, a recent study (26) on both anionically produced (45% syndiotactic triads) and free radically produced (59% syndiotactic triads) poly(tert-butyl methacrylates) indicates a substantially larger characteristic ratio for the former material than for the latter (11.8 versus 10.2). Thus, there appears to be a general trend of decreasing C_∞ with increasing syndiotactic content of polymethacrylates.

Finally, we will briefly remark on the influence of the nature of the Θ solvent on chain dimensions. Results from a recent study (50) of free radically produced PMMA are presented in Table III.

Table III: Specific Solvent Effects on Unperturbed Dimensions of PMMA

Solvent	Theta Temp. (°C)	C_∞
m-xylene	25	7.5
n-butylchloride	35	7.5-7.6
acetonitrile	28	6.6
dipropylketone	35-41	7.1-7.3

The determination of C_∞ is, with care, accurate to within ± 5%. Thus, the characteristic ratio found for PMMA in acetonitrile is definitely smaller than the values found in m-xylene and n-butyl chloride. Intermediate values are found in the theta solvent dipropylketone. Specific solvent effects are well-documented for other polymer/solvent systems (51-55), but the exact nature of these interactions does not appear to be understood.

In summary, the characteristic unperturbed dimensions of polymethacrylates generally increase with: 1) an increase in size of the substituent, and 2) an increase in stiffness of the substituent, and 3)

closer proximity of the center of mass to the main chain. All of these effects increase the barriers of rotation about backbone bonds. Unperturbed dimensions of most polymethacrylates with alkyl side groups increase with temperature. Not much information is available on $d\ln C_\infty/dT$ of other polymethacrylates: such studies would be valuable, Unperturbed dimensions of polymethacrylates increase with an increase in isotactic content and show some dependence on the specific structure of the solvent used in the investigation.

ΑΔΙΑΤΑΡΑΚΤΕΣ ΔΙΑΣΤΑΣΕΙΣ ΠΟΛΥΜΕΘΑΚΡΥΛΙΚΩΝ ΕΣΤΕΡΩΝ ΜΕ ΥΔΡΟΓΟΝΑΝΘΡΑΚΙΚΕΣ ΠΛΕΥΡΙΚΕΣ ΟΜΑΔΕΣ ΚΑΙ ΕΞΑΡΤΗΣΗ ΤΟΥΣ ΑΠΟ ΤΗ ΘΕΡΜΟΚΡΑΣΙΑ

ΠΕΡΙΛΗΨΗ

Γίνεται ανασκόπηση των δημοσιεύσεων που αναφέρονται στις αδιατάρακτες διαστάσεις πολυμεθακρυλικών εστέρων με υδροχοανθρακικές πλευρικές ομάδες. Οι αδιατάρακτες διαστάσεις, επομένως και η ευκαμψία της κυρίας αλυσίδας, εξαρτώνται όχι μόνο από τον όγκο και την ευκαμψία των πλευρικών ομάδων, αλλά και από την απόστασή τους από την κυρία αλυσίδα των πολυμερών. Επίσης επηρεάζονται αισθητά από την τακτικότητα του πολυμερούς, το διαλύτη και σε μερικές περιπτώσεις από τη θερμοκρασία.

REFERENCES AND NOTES

* Portions of this work were previously published by J.W.Mays and N.Hadjichristidis, in *J.Macromol. Sci. ,Revs..*, C28(3&4), 371 (1988).
1. S.W. Shalaby, A.S. Hoffman, B.D. Ratner, and T.A. Horbett, eds., *Polymers as Biomaterials* , Plenum, New York, 1984.
2. E. Chiellini, P. Giusti, C. Migliaresi, and 1. Nicolais, eds., *Polymers in Medicine*, Plenum, New York, 1986.
3. C. B. McArdle, ed., *Side Chain Liquid Crystal Polymers*, Blackie, Glasgow and London, 1989.
4. S.W. Kwolek, P.W. Morgan, and J.R. Shaefgen, Liquid Crystalline Polymers, in *Encyclopedia of Polymer Science and Engineering*, 2nd Ed., J.I. Kroschwitz, ed., Wiley, New York, 1987.
5. P.J. Flory, *Principles of Polymer Chemistry*, Cornell Univ. Press, Ithaca, 1953.
6. P.J. Flory, *J. Chem. Phys.*, 10, 51 (1949).
7. T.G. Fox and P.J. Flory, *J. Phys. Coll. Chem.*, 53 , 197 (1949).
8. B.H. Zimm, *Macromolecules*,13 , 592 (1980).

9. For a recent survey of experimental values see: J.W. Mays, N. Hadjichristidis, and L.J. Fetters, *Macromolecules*, 18 , 2231 (1985).
10. P.J. Flory, *Statistical Mechanics of Chain Molecules*, Wiley-Interscience, New York, 1969.
11. P.J. Flory, *Macromolecules*, 7, 381 (1974).
12. H. Baumann, *J. Polym. Sci.*, Part B, 3 , 1069 (1965). This paper provides a reliable method for treating light scattering data obtained in good solvents.
13. W. Burchard, *Makromol. Chem.*, 50 , 20 (1960).
14. W. H. Stockmayer and M. Fixman, *J. Polym. Sci.*, Part C, 1, 137 (1963).
15. G. Tanaka, *Macromolecules*, 15 , 1028 (1982). This method of treating viscosity data is more reliable than the method of refs. 13 and 14 for estimating unperturbed dimensions from data obtained at large excluded volumes.
16. See, for example: J.M.G. Cowie, *Polymers: Chemistry and Physics of Modern Materials*, International Textbooks, Aylesbury, England, 1973, pp. 213-216.
17. One of several successful correlations between modulus and C_∞ is described by Lin: Y.H. Lin, *Macromolecules*, 20, 3080 (1987).
18. J.W. Mays, S. Nan, Y. Wan, J. Li, and N. Hadjichristidis, *Macromolecules*, submitted.
19. T.G. Fox, *Polymer*, 3 , 111 (1962).
20. S.N. Chinai and R.J. Samuels, *J. Polym. Sci.*, 19 , 463 (1956).
21. S.N. Chinai and R.J. Valles, *J. Polym. Sci.*, 39 , 363 (1959).
22. S.N. Chinai, *J. Polym. Sci.*, 25, 413 (1957).
23. Z.Xu, N. Hadjichristidis, and L.J. Fetters, *Macromolecules*, 17, 2303 (1984).
24. S.N. Chinai and R.A. Guzzi, *J. Polym. Sci.*, 41 , 475 (1959).
25. H.T. Lee and D.W. Levi, *J. Polym. Sci.*, 42, 449 (1960).
26. A. Karandinos, S. Nan, J.W. Mays, and N. Hadjichristidis, *Macromolecules*, in press.
27. F.E. Didot, S.N. Chinai, and D.W. Levi, *J. Polym. Sci.*, 43, 557 (1960).
28. E. Siakali-Kioulafa, N. Hadjichristidis, and J. W. Mays, *Macromolecules*, 22, 2059 (1989).
29. N. Hadjichristidis, M. Devaleriola, and V. Desreux, *Eur, Polym. J.*, 8, 1193 (1972).
30. N. Hadjichristidis and V. Desreux, *J. Macromol. Sci., Chem.*, A6(7), 1227 (1972).
31. N. Hadjichristidis, J. Mays, W. Ferry, and L.J. Fetters, *J Polym. Sci., Polym Phys.* Ed., 22, 1745 (1984).
32. M. Tricot, J. P. Bleus, J.P. Riga, and V. Desreux, *Makromol Chem.*, 175, 913 (1974).
33. L. Gargallo, J. Niezette, and V. Desreux, *Bull, R. Soc. Liege*, 1-2, 82 (1977).
34. L. Gargallo, *Colloid Polym.Sci.*, 253, 288 (1975).
35. R.W. Richards, *Polymer*, 18, 114 (1977).
36. J.W. Mays, N. Hadjichristidis, and J.S. Lindner, *J. Polym. Sci., Polym. Phys. Ed.*, 28, 1881 (1990).
37. J. Niezette, N. Hadjichristidis, and V. Desreux, *Makromol. Chem.*, 177, 2069 (1976).
38. J. B. Alexopoulos, N. Hadjichristidis, and A. Vassiliadis, *Polymer*, 16,386 (1975).

39. J. Alexopoulos and N. Hadjichristridis, *Makromol. Chem.*, 180, 455 (1979).
40. T. Ojeda, D. Radic, and L. Gargallo, *Makromol. Chem.*, 181, 2237 (1980).
41. J.E. Mark, *Rubber Chem. Technol.*, 593 (1973). See also ref.10.
42. A.V. Tobolsky, D. Carlson, and N. Indictor, *J. Polym. Sci.*, 54, 175 (1961).
43. D. Lath and M. Bohdanecky, *J. Polym. Sci., Polym. Lett. Ed.*, 15, 555 (1977).
44. M. Shen, E.H. Circlin, and H.M. Gebhark, *Macromolecules*, 2, 682 (1969).
45. M. Vacatello and P.J. Flory, *Macromolecules*, 19, 405 (1986).
46. P.R. Sundararajan, *Macromolecules*, 19, 415 (1986).
47. R. Jenkins and R.S. Porter, *Adv. Polym. Sci.*, 36, 1 (1980).
48. R. Jenkins and R.S. Porter, *Polymer*, 23, 105 (1982).
49. I. Sakurada, A. Nakajima, O. Yoshizaki, and K. Nakamae, *Kolloid Z.* 186, 41 (1962).
50. O. Quadrat, M. Bohdanecky, and L. Mrkvickova, *Makromol, Chem.*, 182, 445 (1981).
51. T.A. Orofino and J.W. Mickey, *J. Chem. Phys.*, 38, 2512 (1963).
52. T.A. Orofino, *J. Chem Phys.*, 45, 4310 (1966).
53. M. Bohdanecky and D. Berek, *Makromol. Chem., Rapid Commun.*, 6, 275 (1985).
54. J.W. Mays, N. Hadjichristidis, and L.J. Fetters, *Macromolecules*, 18, 2231 (1985).
55. J.W. Mays, N. Hadjichristidis, W.W. Graessley, and L.J. Fetters, *J. Polym. Sci., Polym. Phys. Ed.*, 24, 2553 (1986).

Chimika Chronika, New Series, 20, 51-57 (1991)

SHORT PAPER

SYNTHESIS AND STUDY OF SUBSTITUTED QUINOLINE N-OXIDE ADDUCTS OF TRI(PHENYL)TIN(IV) CHLORIDE

C. BOLOS and A. CHRISTOFIDES

Department of General and Inorganic Chemistry, Aristotelian University of Thessaloniki, Thessaloniki 54006, P.O.B.135, GREECE.

(Received 24.4.89)

SUMMARY

The interaction of triphenyltin chloride with substituted quinoline N-oxides afforded complexes of type $[SnClPh_3L]$ (L=2-MeQNO, 4-MeQNO, 4-ClQNO and 4-NO_2QNO). IR, mass, ^1H, ^{13}C NMR and Mössbauer spectroscopies were used to characterize the complexes and to evaluate the stereochemistry of the ligands around the metal atom. The spectroscopic data showed that the quinoline N-oxides are linked to the metal via the oxygen atom and that the trigonal bipyramidal structure is the most likely for the title complexes.

Key words:Quinoline N-oxide adducts, Triphenyltin(IV) chloride, Spectroscopy IR, mass, ^1H, ^{13}C NMR, Mössbauer.

INTRODUCTION

So far we have been dealing with rhodium(I) complexes bearing substituted quinoline N-oxides as ligands[1-3]. However, we desired to extend our knowledge by investigating the coordination ability of these ligands towards metals from other parts of the periodic table. Our first choise has been platinum(II) which reacted smoothly in the form of Zeise's salt affording yellow air-stable solids[4]. We now report the synthesis and spectral studies of four adducts of $[SnClPh_3]$ with the above ligands.The compound $[SnClPh_3]$ has been chosen for two reasons:

(i) for its tendency to react rather easily with oxygen donor ligands[5] and

(ii) for the scarcity of its adducts incorporating quinoline N-oxides; hitherto, only the adducts of QNO and IQNO have been reported[6].

Our interest in examining as well the effects of the substituents on the coordination ability of quinoline N-oxides towards tin(IV) has also prompted the research described herein, since it has been observed that quinoline N-oxides with electron withdrawing substituents either do not react or react with difficulty[1,3,4]. The spectral study covers also the adduct of IQNO prepared by others[6].

Results and Discussion

Quinoline N-oxides (2-MeQNO, 4-MeQNO, 4-ClQNO and 4-NO_2QNO) react with $[SnClPh_3]$ in 1:1 molar ratio in refluxing chloroform affording air-stable, coloured complexes. The elemental analyses (C,H,N and Cl) as well as the melting points show that the compounds (I-IV) are received in pure forms and they do not need recrystallization. Analytical results, melting points and yields are given in Table 1. It is worth to note in this

TABLE I. Analytical Data, Melting Points, Colours and Yields of Triphenyltin(IV) Compounds.

COMPOUND	%C		%H		%N		%Cl		M.P. °C	Colour	Yield
	Found	Calc.	Found	Calc.	Found	Calc.	Found	Calc.			
I $[SnClPh_3 2\text{-MeQNO}]$	61.55	(61.74)	4.37	(4.41)	2.50	(2.57)	6.45	(6.52)	145-7	Off-White	55
II $[SnClPh_3 4\text{-MeQNO}]$	61.60	(61.74)	4.40	(4.41)	2.55	(2.57)	6.40	(6.52)	160-2	Off-White	60
III $[SnClPh_3 4\text{-ClQNO}]$	57.30	(57.38)	3.70	(3.72)	2.50	(2.48)	12.50	(12.57)	123-5	Off-White	58
IV $[SnClPh_3 4\text{-}NO_2\text{QNO}]$	56.00	(56.33)	3.60	(3.65)	4.80	(4.87)	6.15	(6.17)	93-5	Yellow	78

point that well developed crystals of the new complexes suitable for investigation by X-ray diffraction can be grown by slow evaporation of the solvent.

Complexes (I-IV) appear to be five coordinated so the structure either of trigonal-bipyramid (TBP) or square pyramid (SP) can be attained by them[5,7,8,9]. The available spectroscopic data are in favour of the former structure. In particular, the IR spectra exhibit bands assignable to ν(N-O) shifted almost in all complexes to lower wave numbers as compared to those of the free ligands, the donor interaction being stronger in I[5], Table 2. However, the situation concerning the band due to δ(N-O) is opposite, since it shows a positive shift and only in the spectrum of

TABLE II. The Most Important Infrared Bands of Triphenyltin(IV) Complexes

COMPOUND	IR Bands(cm^{-1})					
	ν(N-O)	Δν	δ(N-O)	Δδ	ν(M-O)	ν(M-Cl)
2-MeQNO	1204	-	810	-	-	-
[$SnClPh_3$2-MeQNO]	1190	-14	815	+5	450	330
4-MeQNO	1206	-	823	-	-	-
[$SnClPh_3$4-MeQNO]	1201	-5	825	+2	450	330
4-ClQNO	1302	-	820	-	-	-
[$SnClPh_3$4-ClQNO]	1295	-7	825	+5	450	335
4-NO_2QNO	1300	-	840	-	-	-
[$SnClPh_3$4-NO_2QNO]	1295	-5	830	-10	445	325

IV the respective band is shifted to lower wave numbers. Moreover, this shift caused by complexation is slight and has previously been observed by others[10-12]. No appreciable differences were observed in the IR spectra of I-IV, which could be due to the influence of certain substituents.

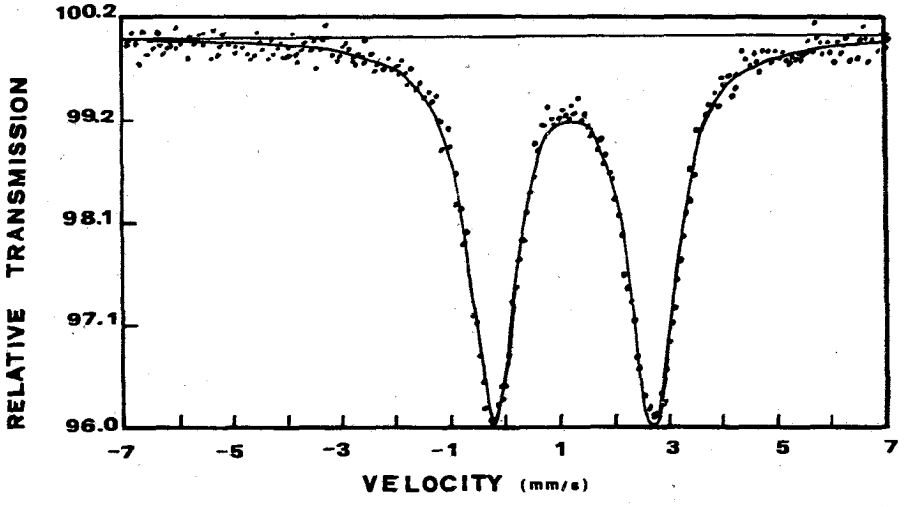

FIG. 1. *Mössbauer spectrum of* [$SnClPh_3$·IQNO] *at 78°K. Isomeric shift: 1.27 mm.s^{-1}, relative to $CaSnO_3$.*

^{119}Sn Mössbauer spectrum of [$SnClPh_3$·IQNO] (Fig. 1) shows quadrupole splitting (QS) 2.94 mm.s^{-1}, this value being typical for TBP structu-

re having the equatorial positions occupied by the phenyl groups[5]. Furthermore, this value being much higher than that (1.86 $mm \cdot s^{-1}$) of [$SnPh_3$(2-SPyO)] addopting the SP structure[9], rules out this configuration from the investigated complexes. The value of the ratio QS/IS, 2.31, argues also in favour of the TBP structure, since it is greater than ca.2.1 and this in turn means coordination number larger than four for di- and triorganotin(IV) derivatives, as it was suggested earlier[13].Moreover, the quadrupole splitting(QS) of [$SnClPh_3 \cdot IQNO$] is similar to that of [$SnBr(p\text{-tolyl})_3QNO$] suggesting similar configurations for both compounds as M.A. Mullins et al.[14] observed earlier for other tin(IV) pentacoordinated species.

Taking into account the above discussion and especially the X-ray crystal data of the quinoline N-oxide adduct of tri(p-tolyl)tin bromide[5] showing that the coordination geometry at tin is a TBP, we propose for the investigated complexes the structure shown below:

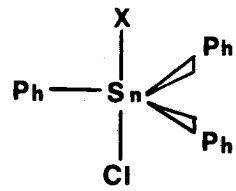

X

I 2-MeQNO
II 4-MeQNO
III 4-ClQNO
IV 4-NO_2QNO

Additional evidence for the above structure is provided also by the ^{13}C NMR spectra of III and IV, the main feature of which are the resonances in the range 139-127 ppm, indicating four nonequivalent carbon atoms of the phenyl rings. The ipsocarbon atoms of the phenyl rings show a small down field shift, suggesting the formation of trans trigonal bipyramidal adduct[5,15]. The ^{13}C NMR data of the complexes studied are reported in Table 3. Unfortunately, owing to solubility reasons we have been unable to take the spectra of the rest complexes. Moreover,we could

TABLE III. ^{13}C NMR Data for the Organotin Moiety in two Triphenyltin(IV) Compounds in Concentrated $CDCl_3$ Solution.

Compound	δ(Ci)[a]	δ(Co)	δ(Cm)	δ(Cp)	^1J	^2J	^3J	^4J
$[SnClPh_3 4\text{-}ClQNO]$	139.0	136.2	128.9	129.9	–[b]	48.0	66.0	12.0
$[SnClPh_3 4\text{-}NO_2QNO]$	137.6	136.1	127.1	130.4	–	48.5	64.0	14.0
$[SnClPh_3]$[c]	137.1	136.0	129.0	130.4	614.3	50.0	64.5	13.4

[a] i(ipso),o(ortho),m(meta),p(para);Coupling Constants refered to $J(^{119}Sn\text{-}^{13}C)$.

[b] Coupling Constants cannot be evaluated from data.

[c] Ref. 5.

not see the $^1J(^{119}Sn\text{-}^{13}C)$, which would be another indication for the proposed geometry, because that was beyond the range of the available spectrometer.

The ^1H NMR spectra of I and II exhibit all the expecting peaks without any appreciable shift relative to the uncomplexed tin(IV) moiety or to free substituted quinoline N-oxide.

The mass spectrum of $[SnClPh_3 \cdot IQNO]$ shows no peak assignable to molecular ion. However, peaks due to $[SnClPh_3]$ and its fragments as well as to IQNO were detected.

The low values of molar conductances show no ionic character.

EXPERIMENTAL

Physical measurements

Elemental analyses (C,H,N) were obtained with a Perkin-Elmer 240 Elemental Analyser. Chlorine was determined by combustion after Schöninger, followed by titration with silver nitrate. Infrared spectra were recorded in the 4000-200 cm^{-1} region on a Perkin-Elmer 1430 spectrophotometer using KBr pellets. Mass spectra were measured on a RMU-6L Hitachi Perkin-Elmer mass spectrometer with ionization source of T-2p type operating at 70eV. Melting points were determined with a Büchi apparatus and are uncorrected. ^1H NMR spectra were measured on a Bruker AW-80 in $CDCl_3$. ^{13}C NMR spectra were taken on a Fourier Transform Varian CFT 20 spectrometer and $CDCl_3$ was used as solvent; the solutions were approximately 0.1g·ml^{-1}. Mössbauer spectrum was obtained with a conventional constant accelerator spectrometer. The source was 25mCi of ^{57}Co in a copper matrix.

Starting Materials

All solvents were of reagent grade and were used without further purification in synthetic work. The ligands were prepared and recrystallized as previously reported[3]. Triphenyltin chloride was used as obtained from Merck-Schuchardt.

Preparation of Complexes

All these were prepared in a similar manner; the following synthesis is representative.

$[SnClPh_3 \cdot 2MeQNO]$

An equimolar mixture of triphenyltin chloride (0.385g., 1mmol) and 2-methylquinoline N-oxide (0.159g., 1mmol) was refluxed in chloroform (50ml) for 1h. Concentration of the resulting solution to a small volume (10ml) yielded off-white solid, which was filterred off, washed with ether and dried under vacuum. ^1H NMR spectrum ($\{^2H_1\}$ chloroform), 2.43 (s, 3H, Me), 7.09-8.52ppm (m, 23H, Ph and 2-MeQNO).

The ^1H NMR spectrum ($\{^2H_1\}$ chloroform) of II showed resonances at 2.60 (s, 3H, Me), 6.85-8.60ppm (m, 23H, Ph and 4-MeQNO).

Περίληψη "Σύνθεση και μελέτη των ενώσεων προσθήκης των υποκατεστημένων κινολινο N-οξειδίων με τριφαινυλοχλωροκασσίτερο(IV)"

Η αντίδραση του τριφαινυλοχλωροκασσίτερου(IV) με υποκατεστημένα κινολινο N-οξείδια έδωσε σύμπλοκα του γενικού τύπου $[SnClPh_3L]$, (L=2-MeQNO 4-MeQNO, 4-ClQNO και 4-NO_2QNO).

Η μελέτη της δομής των συμπλόκων έγινε με διάφορες φασματοσκοπικές μεθόδους (IR, mass, ^1H, ^{13}C NMR και Mössbauer) σε συνδυασμό με τη μοριακή αγωγιμότητα. Τα αποτελέσματα της μελέτης αυτής έδειξαν ότι τα κινολινο N-οξείδια συναρμόζονται με το μέταλλο μέσω του ατόμου του οξυγόνου και η πιο πιθανή δομή των συμπλόκων είναι αυτή της τριγωνικής διπυραμίδας.

References

1. Christofides, A. and Labrinou, I., *Inorg. Chim. Acta.*, 99, 155 (1985).
2. Christofides, A., Drigas, D., Tourka, E., *Inorg. Chim. Acta*, 126, 95 (1987).
3. Christofides, A., *Inorg. Chim. Acta*, 133, 29 (1987).
4. Christofides, A. and Stiakaki, M.A., *"7th Fechem Conference on Organometallic Chemistry, Toledo, 1987"* Real Sosiedad, Espanola de Quimica, Toledo, 1987, Abstracts EV II, P.25.
5. Das V.C. Keong, V.G.K., Weng, N.G.S. and Wei, C., *J. Organometallic Chemistry*, 311, 289 (1986) and references therein.
6. Srivastava, T.N., Srivastava, P.C. and Gaur, J.S., *Indian J. Chem.*,

Sect.A, 17A, 142 (1979).

7. Pelicci, C., Pelicci, G. and Tarasconi, P., *J. Organom. Chem.*, 124, 151 (1977).
8. Pelicci, G., *Inorg. Chim. Acta*, 24, L31 (1977).
9. Ng, S.W., Wei, C., Das, V.G.K and Mak, T.C.W., *J. Organom. Chem.*, 334, 283 (1987).
10. Kawasaki, Y., Hori, M. and Venaka, K., *Bull. Chem. Soc. (Japan)*, 40, 2463 (1967).
11. Kida, S., Quagliano, J.V., Walmsley, J.A. and Tyree, S.K., *Spectrochimica Acta*, 19, 189 (1963).
12. Kakiuti, Y., Kida, S. and Quagliano, J.V., *Spectrochim. Acta*, 19, 201 (1963).
13. Herber, R.H., Stöckler, H.A. and Reichle, W.T., *J. Chem. Phys.*, 42, 2447 (1965).
14. Mullins, M.A. and Curran, C., *Inorg. Chem.*, 7, 2584 (1968).
15. Lŷcka, A., Holeček, J., Nabvornik, M. and Handlir, *J. Organom. Chem.*, 280, 323 (1985).

Chimika Chronika, New Series, 20, 59-64 (1991)

SHORT PAPER

THE TERNARY SYSTEM ARSENIOUS ACID-n-TETRABUTYLAMMONIUM HYDROXIDE-WATER AT +4°C

GERASIMOS M.TSIVGOULIS and PANAYIOTIS V.IOANNOU*
Department of Chemistry, University of Patras, Patras, Greece

(Received April 22, 1991)

SUMMARY

The system $H_3AsO_3/n\text{-}Bu_4NOH/H_2O$ at +4°C has been studied. The solid phases found were $n\text{-}Bu_4NOH.(8.5 \pm 1.5)H_2O$, $n\text{-}Bu_4NOH.(21.1 \pm 3.8)H_2O$, and $n\text{-}Bu_4NOH.H_3AsO_3.38H_2O$. In the absence of crystallographic data the exact composition and the structures of the clathrate hydrates are not known.

Key words: Arsenious acid, n-tetrabutylammonium hydroxide, clathrate hydrates.

INTRODUCTION

Well defined salts of H_3AsO_3 with simple inorganic cations are difficult to obtain in the solid state[1,2] while those with organic cations, to the best of our knowledge, have not been prepared. Salts of H_3AsO_3 with lipophilic organic cations, e.g. $(R_4N)_3AsO_3$, may be useful in running the Meyer reaction[3] in non-hydroxylic solvents, a task not hitherto realized.

Being unable to prepare by extraction a salt of type $Q_{3-x}H_xAsO_3$ (Q^+ : abbreviation for $n\text{-}Bu_4N^+$) we studied the ternary system $H_3AsO_3\text{-}QOH\text{-}H_2O$ at +4°C, using a modified Schreinemakers' wet residue method,[4] in order to find out which solid phases crystallize.

EXPERIMENTAL

Fresh aqueous n-tetrabutylammonium hydroxide (~42%) (Merck and Ferak) was used. Diluted samples were prepared under nitrogen and standardized with standard hydrochloric acid. Arsenic trioxide was A.R. grade (Ferak) and the water

was doubly distilled.

To a weighed amount of As_2O_3, a known volume of aqueous QOH was added and the clear solution was diluted with known weight of water under nitrogen. From the density of the QOH solution and calculating the water consumed for the reaction $As_2O_3 + 3H_2O \rightarrow 2H_3AsO_3$ the exact initial composition of each sample was known.

The stoppered samples were left undisturbed at $+4.0 \pm 0.5^{o}C$ for crystallization. When a sample did not start crystallizing after 24h, seed crystals were formed by brief cooling of the sample at $-20^{o}C$ and then was left at $+4^{o}C$. Preliminary experiments showed that equilibrium has been reached in less than 4 days, but the samples were analysed after 10 days at $+4^{o}C$.

Liquid phase samples were withdrawn with a pipette, weighed, diluted to a known volume with water and aliquots were analysed, at least twice, for As(III) and Q^+. As(III) was determined titrimetrically with standard $KBrO_3$;[5] QOH did not interfere with the determination. The relative errors of the titrations were ±0.1% and ±1.0% at 0.1N and 0.01N, respectively, Na_3AsO_3, NaQ_2AsO_3 or Q_3AsO_3. Q^+ was determined nephelometrically as $Q^+(C_6H_5)_4B^-$ using a Hach, model 2100 A, turbidimeter. Eight replicates $1.03 \pm 0.02 \times 10^{-5}M$ aqueous QOH gave $\bar{x} \pm SD$ $1.02 \pm 0.01 \times 10^{-5}M$ (coefficient of variation, CV, 0.98%).[6]

The intersection point of each tie-line with the QOH-$-H_2O$ side of the triangle was found algebraically.[7]

RESULTS AND DISCUSSION

We chose the known initial composition and the analysis of the liquid phase over the classical Schreinemakers' wet residue method[4] because the crystals could not be freed from the surplus liquid phase[7] without melting. The drawback of graphically extrapolating a tie-line defined by these two more closely spaced points was partially offset by using algebraic extrapolation.[7]

Figure 1 shows the general regions of the system QOH-

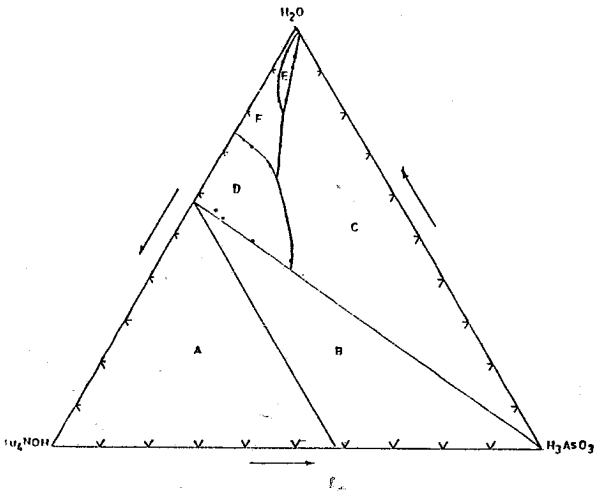

FIG.1. *The F region of the ternary system n-Bu_4NOH-H_3AsO_3-H_2O at +4°C is amenable for study.*

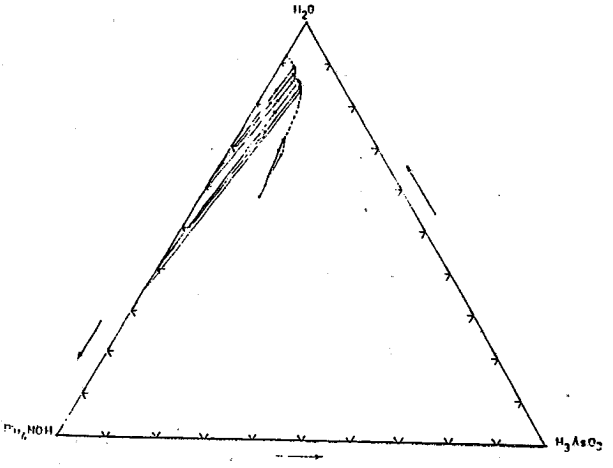

FIG.2. *Phases formed in the ternary system n-Bu_4NOH-H_3AsO_3-H_2O at +4°C.*

-H_3AsO_3-H_2O. Region A cannot be studied because the maximum concentration of QOH is ~42% w/w. The line H_3AsO_3 —42% QOH represents the addition of pure H_3AsO_3 to 42% QOH and therefore region B cannot be studied. Samples in region C left As_2O_3 undissolved, solutions at 25°C with initial compositions falling in D solidified completely at +4°C while those in E gave no crystals at +4°C. Therefore the only part of the isothermal phase diagram amenable to study is region F.

In Table I the initial compositions, the results of the analyses and the composition of the solid phases are listed and in Figure 2 representative points are plotted. The intersection points on the QOH-H_2O line are grouped between two

TABLE I. Analyses and composition of the solid phases of the system n-$Bu_4NOH/H_3AsO_3/H_2O$ at +4°C.

Initial composition, weight %		Composition of liquid phase, weight %		Composition of solid phase	
n-Bu_4NOH	H_3AsO_3	n-Bu_4NOH	H_3AsO_3		
10.52	10.40	30.44	11.52	n-$Bu_4NOH/H_3AsO_3/H_2O$	1.15/1/38.2
10.09	9.80	20.43	10.04	"	1.15/1/38.2
22.28	5.66	8.95	7.34	n-Bu_4NOH/H_2O	1/7.0
21.39	5.42	9.19	7.04	"	1/8.7
17.36	4.41	8.71	5.32	"	1/9.9
15.00	3.81	10.33	4.49	"	1/20.3
11.79	3.00	6.95	3.43	"	1/17.2
8.71	2.21	6.15	2.38	"	1/20.5
22.69	3.85	6.14	6.37	"	1/15.6
17.21	2.95	9.86	3.89	"	1/21.5
16.64	2.82	8.53	3.82	"	1/21.9
14.03	2.39	8.18	2.98	"	1/23.9
12.44	2.12	7.78	2.57	"	1/28.0

ranges, 67-59% QOH and 48-34% QOH, giving 8.5 ± 1.5 and 21.1 ± 3.8 molecules of water per QOH molecule. The spreading of intersection points is reasonable,[8] but due to the great difference in the molecular weights of QOH and H_2O (259 and 18 respectively) it is very difficult, in the absence of crystallographic data (Prof. G.A.Jeffrey' personal communication), to decide on the exact composition of the precipitated clathrates. Fowler et al.[9] evaporating aqueous solutions of QOH obtained the hydrates $QOH.xH_2O$ (x = 31, 4 and 2) while Aladko et al.[10] by crystallizing aqueous solutions of QOH obtained hydrates with x = 28 and 32. Zagórski[11] commented on the variability of the water content of QOH hydrates and he also observed differences in the stoichiometry in different parts of large crystals.

Two samples gave a solid phase with a composition $QOH/H_3AsO_3/H_2O$ 1.15/1/38.2 which corresponds to $Q^+H_2AsO_3^-.39H_2O$. It is not unreasonable to suppose that the entities $[OH^-.3H^+.AsO_3^{3-}.xH_2O]$ form a clathrate-like cage to enclose the Q^+ cation, but in the absence of single crystal X-ray data the structure of the cage[12] remains speculative.

In a study of the system $Na_2O/As_2O_3/H_2O$, at +6°C, four phases, all containing As(III), have been identified.[2] These were : $Na_2H_2As_4O_8$, $NaAsO_2.4H_2O$, $Na_2HAsO_3.5H_2O$ and $Na_5(HAsO_3)(AsO_3).12H_2O$. Comparing the two systems, it is apparent that in the presence of the n-tetrabutylammonium cation the clathrate hydrates of this cation preferentially precipitate.

ΠΕΡΙΛΗΨΗ. Το σύστημα εκ τριών συστατικών αρσενικώδες οξύ-
υδροξείδιο του n-τετραβουτυλαμμωνίου- ύδωρ στους
+4°C

Μελετήθηκε το σύστημα $H_3AsO_3/n\text{-}Bu_4NOH/H_2O$ στους +4°C. Βρέθηκαν τρεις στερεές φάσεις : $n\text{-}Bu_4NOH.(8.5 \pm 1.5)H_2O$, $n\text{-}Bu_4NOH.(21.1 \pm 3.8)H_2O$ και $n\text{-}Bu_4NOH.H_3AsO_3.38H_2O$. Απουσία κρυσταλλογραφικών δεδομένων, η ακριβής σύσταση και οι δομές των ενώσεων εγκλωβισμού υδριτών δεν είναι γνωστές.

ACKNOWLEDGEMENTS

The financial support by the General Secretariat of Research and Technology, Ministry of Industry, Energy and Technology is gratefully acknowledged. We thank Professor G.A.Jeffrey, University of Pittsburgh,U.S.A., for helpful discussions.

REFERENCES

1. Jander, G. and Hofmann, H., *Z.Anorg.Allg.Chem.*, 296, 134 (1958).
2. Sheldrick, W.S. and Häusler, H.- J.,*Z.Anorg.Allg.Chem.*, 549, 177 (1987).
3. Doak, G.O. and Freedman, L.D., *Organometallic Compounds of Arsenic, Antimony and Bismuth*, pp.17-62, Wiley, New York (1970).
4. Maron, S.H. and Prutton, C.F., *Principles of Physical Chemistry*, 4th Ed., p.385, MacMillan, New York (1965).
5. Vogel, A.I., *Textbook of Quantitative Inorganic Analysis*, 4th Ed., revised by J.Bassett, R.C.Denney, G.H.Jeffery and J.Mendham, p.392, Longman, London (1979).
6. Tsivgoulis, G.M. et al., Unpublished results.
7. Findlay, A., *The Phase Rule*, 9th Ed. by A.N.Cambell and N.O.Smith, pp. 378-380, Dover, New York (1951).
8. Buettner, J.P. and Jache, A.W., *Inorg.Chem.*, 2, 19 (1963).
9. Fowler, D.L.,Loebenstein, W.V.,Pall, D.B. and Krauss, C.A., *J.Am.Chem.Soc.*, 62, 1140 (1940).
10. Aladko, L.S., Dyadin, Yu.A., Polyanskaya, T.M. and Terekhova, I.S., *Izv.Sib.Otd.Akad.Nauk. SSSR, Ser.Khim.Nauk*, 41 (1977); *Chem.Abs.*, 86, 178208n (1977).
11. Zagórski, Z.P., *J.Phys.Chem.*, 90, 957 (1986).
12. Geffrey, G.A. and McMullan, R.K., *Prog.Inorg.Chem.*, 8, 43 (1967).

CHIMIKA CHRONIKA, *NEW SERIES*

CONTENTS

March 1991 Volume 20 No 1